

Challenges and pitfalls of inferring microbial growth rates from lab cultures

Ana-Hermina Ghenu^{*1,2,3}, Loïc Marrec^{†2,3}, and Claudia Bank^{1,2,3}

¹Instituto Gulbenkian de Ciência, Rua da Quinta Grande 6, Oeiras, 2780-156, Portugal

²Institut für Ökologie und Evolution, Universität Bern, Baltzerstrasse 6, CH-3012 Bern, Switzerland

³Swiss Institute of Bioinformatics, 1015 Lausanne, Switzerland

June 24, 2022

Abstract

After more than 100 years of generating monoculture batch culture growth curves, microbial ecologists and evolutionary biologists still lack a reference method for inferring growth rates. Our work highlights the challenges of estimating the growth rate from growth curve data and shows that inaccurate estimates of growth rates significantly impact the estimated relative fitness, a principal quantity in evolution and ecology. First, we conducted a literature review and found which different types of methods are currently used to estimate growth rates. These methods differ in the meaning of the estimated growth rate parameter. Kinetic models estimate the intrinsic growth rate μ whereas statistical methods – both model-based and model-free – estimate the maximum *per capita* growth rate μ_{\max} . Using math and simulations, we show the conditions in which μ_{\max} is not a good estimator of μ . Then, we demonstrate that inaccurate absolute estimates of μ is not overcome by calculating relative values. Importantly, we find that poor approximations for μ sometimes lead to wrongly classifying a beneficial mutant as deleterious. Finally, we re-analyzed four published data-sets using most of the methods found by our literature review. We detected no single best-fitting model across all experiments within a data-set and found that the Gompertz models, which were among the most commonly used, were often among the worst fitting. Our study provides suggestions for how experimenters can improve their growth rate and associated relative fitness estimates and highlights a neglected but fundamental problem for nearly everyone who studies microbial populations in the lab.

1 Introduction

Measuring batch culture growth curves is a common method used by nearly all who work with single-celled organisms in the laboratory. Growth curves allow experimenters to readily

*Co-first and co-corresponding author: hermina.ghenu@gmail.com

†Co-first and co-corresponding author: loic.marrec@iee.unibe.ch

25 measure population phenotypes, like the dynamics and efficiency of growth in particular en-
26 vironments, for microscopic organisms whose individual cell phenotypes are often laborious
27 or expensive to quantify. The growth rate is an especially important trait for evolutionary
28 microbiologists and microbial ecologists. The growth rate is important because it is related
29 to fitness in population biology, it is used to estimate the number of generations a microbial
30 culture has been growing for (e.g., Wein and Dagan 2019), it is more responsive to selection
31 than other traits in microbial evolution experiments (Wahl and Zhu, 2015), and it is central
32 in describing competition for limited resources (Miller et al., 2005; Bernhardt et al., 2020).
33 Overall, growth curves are commonly used because they are easy to obtain, have been used
34 for a long time, and usually give consistent results within an experiment. The importance of
35 growth curves is only increasing in the age of high-throughput experimental screens of micro-
36 bial populations, from which conclusions are drawn about responses to ecological challenges,
37 to antimicrobial drugs, and about optimal strains for agricultural purposes. Nevertheless,
38 despite the popularity of gathering growth curve data and the proliferation of methods for
39 extracting growth parameters from said data, it is not clear what is the best method for
40 estimating values of interest for these data.

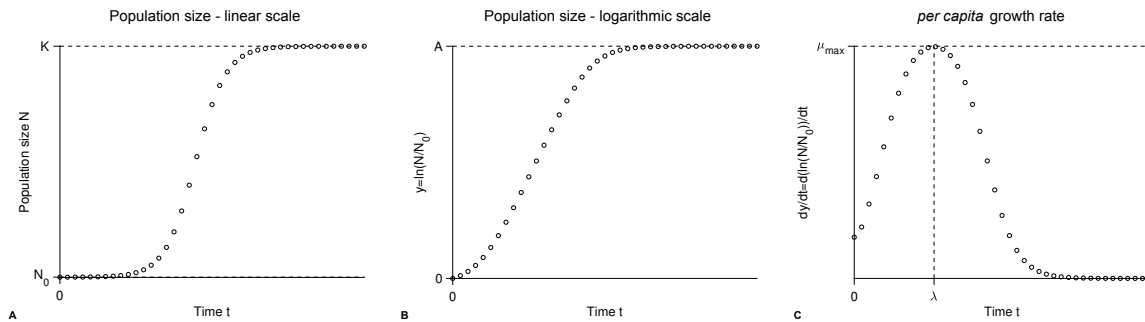


Figure 1: **A schematic illustration of the same simulated batch culture population growth curve, plotted in three different ways.:** **A)** Population size N versus time t . The quantity K corresponds to the carrying capacity and N_0 to the initial population size. The initial population density or fraction is given by N_0/K . **B)** Logarithm of the population size divided by the initial population size $y = \ln(N/N_0)$ versus time t . Note that in other publications the quantity $\ln(N/N_0)$ is sometimes denoted as y . The quantity $A = \ln(K/N_0)$ is the logarithm of the fold increase over the initial population size at carrying capacity. **C)** First derivative of the logarithm of the population size divided by the initial population size $dy/dt = d \ln(N/N_0)/dt$ versus time t . The function dy/dt may be interpreted as the *per capita* growth rate. The quantity μ_{\max} is the *per capita* maximum growth rate and λ the lag phase duration.

41 The idea behind the batch culture growth curve is simple: inoculate a sterile culture
42 medium with a small number of individuals N_0 and track the increase in population size
43 over time using any available method to estimate population size (e.g., colony forming units,
44 optical density, microscopy cells counts, flow cytometry). An idealized growth curve is shown
45 in Figure 1, in which each panel shows the same simulated data but with a different y-axis.
46 When an experimenter assesses a growth curve, what they may first observe is perhaps a “lag
47 phase” with little growth. Then, they will *always* observe a phase of rapid growth, alternately
48 called the “log phase” or “linear phase” by different researchers, in which the growth is linear

49 when shown with the y-axis on a log-scale (Figure 1B). Figure 1C shows the first derivative of
50 Figure 1B: in other words, the instantaneous *per capita* growth rate. The fastest growth rate
51 is usually reached during the “log/linear phase” (Figure 1C; Monod 1949). Then, this phase
52 may be followed by more decelerations and subsequent accelerations under diauxic/diphasic
53 growth conditions (not shown or further discussed herein). Eventually the population growth
54 slows down to halt at the “stationary phase”, reaching the final carrying capacity (denoted
55 K in linear-scale, Figure 1A, or A in log-scale, Figure 1B) when all the usable resources are
56 depleted from the batch culture.

57 Growth curves are often used to estimate the *per capita* growth rate and fitness. The
58 *per capita* growth rate is important in population biology because it is used to calculate the
59 growth of a mutant strain as compared to a wild-type strain: this is the relative growth rate, or
60 the relative fitness (w). The relative fitness is particularly important in evolutionary biology
61 since it classifies a mutant as deleterious ($w < 1$), neutral ($w = 0$) or beneficial ($w > 1$)
62 with respect to natural selection. Indeed, when the relative fitness is greater than 1, the
63 mutant reproduces faster than the wild-type, and conversely when w is less than 1. Although
64 there is still discussion in the field about whether the relative growth rates measured from
65 monoculture growth curves are predictive of competitive fitness (Concepción-Acevedo et al.,
66 2015; Ram et al., 2019), many biologists use the growth rate as a measure of fitness (e.g.,
67 Knopp and Andersson 2018).

68 Microbial batch culture protocols have been used for over 100 years in microbiology (e.g.,
69 Slator 1916) and population ecology (e.g., Carlson 1913), and remain a mainstay of experi-
70 mental evolution and ecology. During this time, many experimental protocols (Delaney et al.,
71 2013; Hall et al., 2014; Stevenson et al., 2016; Kurokawa and Ying, 2017) and estimation
72 methods (Zwietering et al., 1990; Baranyi and Roberts, 1994; Jung et al., 2015) have been
73 developed for this type of data. Since the early 1990s, automated plate readers that incubate
74 and periodically scan the opacity of the cultures growing in the microwells have simplified
75 the process of gathering data for hundreds of bacterial populations simultaneously growing in
76 (relatively) homogeneous batch culture environments. Sources of inconsistency, like the batch
77 effect (Blomberg, 2011), can be mitigated, for example by growing all cultures of interest on
78 the same day(s), in order to arrive at consistent data. Nevertheless, despite the long tradi-
79 tion and good recommendations for setting up experiments, programs and papers detailing
80 methods for estimating growth rates (and other growth parameters) from this data continue
81 to be published and highly sought after. Many of these estimation methods are implementa-
82 tions of classical models (e.g. Sprouffske and Wagner 2016; Petzoldt 2020). This shows that
83 also after 100+ years of generating growth curve data, microbial ecologists and evolutionary
84 biologists are still struggling to find the best way of estimating the growth rate from their data.

85
86 The main goal of our paper is to demonstrate that there are significant limitations to ex-
87 isting methods for using batch culture growth curve data to estimate the intrinsic growth rate
88 μ , which is the fastest *per capita* number of divisions per time unit possible when the cell’s
89 resources are limitless or otherwise optimal. These limitations impact the calculation of quan-
90 tities of interest such as the selection coefficient and the relative fitness. We first take stock
91 of how the community currently analyzes growth curve data by semi-quantitatively reviewing
92 the literature to survey which methods are used in evolution and ecology. After explaining
93 different approaches for modelling growth curves, we then use math and simulations to show
94 that many of the currently used approaches are inappropriate for accurately estimating the

95 intrinsic growth rate μ . We quantify the errors for the intrinsic growth rate μ when the max-
96 imum attained growth rate μ_{\max} is used as an estimator and the generating model is known.
97 Next, we present the limited set of conditions in which an exponential approximation can
98 be used for estimating μ . Importantly, we demonstrate that using inaccurate estimates of μ
99 to estimate the relative fitness often leads to inaccurate fitness estimates and sometimes to
100 wrongly classifying a beneficial mutation as deleterious in some cases. Finally, we apply our
101 theoretical insights to previously published data and show that both absolute and relative
102 growth rate estimates may vary greatly depending on the method. Overall, we present a
103 systematic evaluation of different methods, with recommendations for best practices.

104 2 Results & Discussion

105 2.1 Literature review: How does the community analyze the data?

106 We reviewed 50 papers from evolution and ecology that estimated growth curves for all types
107 of microbial data (see Table S1 and Methods section). Most of the data (90%) were acquired
108 by an automated microplate reader tracking optical density (OD) over time. Other data
109 types included cell counts or fluorescent yields over time. Several papers (6%) did not report
110 the starting inoculum size. Of those papers that reported the inoculum size, 52% used a
111 fixed absolute initial population size (\widehat{N}_0) for inoculation whereas 44% used a constant initial
112 population fraction ($\widehat{N}_0 = \widehat{K} \times \text{dilution factor}$), which we hereafter refer to as the dilution
113 fraction. A constant dilution fraction means that stationary-phase cultures, whose populations
114 are at their carrying capacity, K , were diluted by a constant dilution factor (e.g., 1/1000 \times).
115 This means that for experiments with a constant dilution fraction the absolute population
116 size of the inoculum, N_0 , differed between strains/treatments when the carrying capacities,
117 K , were different. For experiments using a constant dilution fraction, the reported dilution
118 factor varied between 10^{-4} to 10^{-1} with a geometric mean value of $10^{-2.37}$.

119 We found that the growth rate was by far the most commonly estimated growth parameter
120 (94% of all papers reviewed). The other estimated growth parameters were: the carrying
121 capacity (44%), the lag time (34%), and the area under the curve (AUC; 12%). The growth
122 rate was usually reported as an absolute value for each strain/treatment. Moreover, 24% of
123 papers estimated the relative growth rate, or relative fitness, of different strains as compared
124 to the wild-type.

125 Methods that explicitly fit a model of population growth were used about as often as
126 “model-free” or “nonparametric” approaches (i.e., methods that do not require a model;
127 Figure 2A). One particular model-free approach, the “Easy Linear” method, was especially
128 popular (right doughnut chart of Figure 2A): it was used in about a third of all papers. When
129 models *were* used, only one model was usually reported to have been fit (left doughnut chart
130 of Figure 2A).

131 We classified the growth curve analysis methods as either kinetic or statistical (Figure
132 2B). A kinetic model is a mechanistic representation that allows researchers to simulate the
133 underlying process. In contrast, a statistical approach enables researchers to describe and
134 quantify the pattern of interest but without simulating the underlying process. We found
135 that statistical approaches were used more often than kinetic models (Figure 2B). The most
136 popular methods within the statistical approach were the various model-free methods (right
137 doughnut of Figure 2B). The logistic model was by far the most popular kinetic model used

138 (left doughnut of Figure 2B). Depending on its equation, the Gompertz model is either a
139 statistical or a kinetic model (table 1); however, we found that the kinetic Gompertz model
140 was never fitted whereas the statistical Gompertz model was popular (18% of all papers and
141 28% of all statistical methods used).

142 We found that many growth curve experimental methods, data, and analyses do not yet
143 conform with recommendations for reproducible research (e.g., Wilkinson et al. 2016; Munafò
144 et al. 2017). Over 10% of the papers reviewed reported insufficient information about how
145 growth curves were analyzed and therefore could not be classified for Figure 2. Some highly-
146 cited papers (e.g. Gullberg et al. 2011; Trindade et al. 2012) neither cited an established
147 method nor included sufficient description of their *ad hoc* methods for estimating growth
148 rates (see table S1). Beyond reporting of experimental methods, the data-set itself was often
149 not shared: about half (46%) of all papers do not show any figures of nor provide any of the
150 growth curve data (see table S1). 40% of papers provided plots of at least a subset of the
151 growth curves and 14% of all papers published their raw growth curve data.

152 Our finding from Figure 2 that $\sim 13\%$ of articles provide insufficient information regarding
153 their growth curve analysis methods likely *underestimates* the magnitude of the problem.
154 This is because we found articles for inclusion in the review by searching among the citations
155 to previously published growth curve analysis methods papers (see methods). Therefore,
156 most of the papers we included cited an established method for analyzing growth curve data.
157 Hopefully these issues of methods under-reporting will improve as scientists become more
158 knowledgeable about recommendations for open science and data management (Wilkinson
159 et al., 2016; Munafò et al., 2017).

160 Our finding of insufficiently reported information regarding the analysis of growth curves
161 corroborates previous concerns about the lack of a standard method for growth curve analysis
162 (Fernandez-Ricaud et al., 2016). The remainder of our article discusses different methods
163 for analyzing growth curves and, thus, will hopefully contribute to an increased appreciation
164 of why it is important to provide sufficiently detailed methodological information on data
165 analyses.

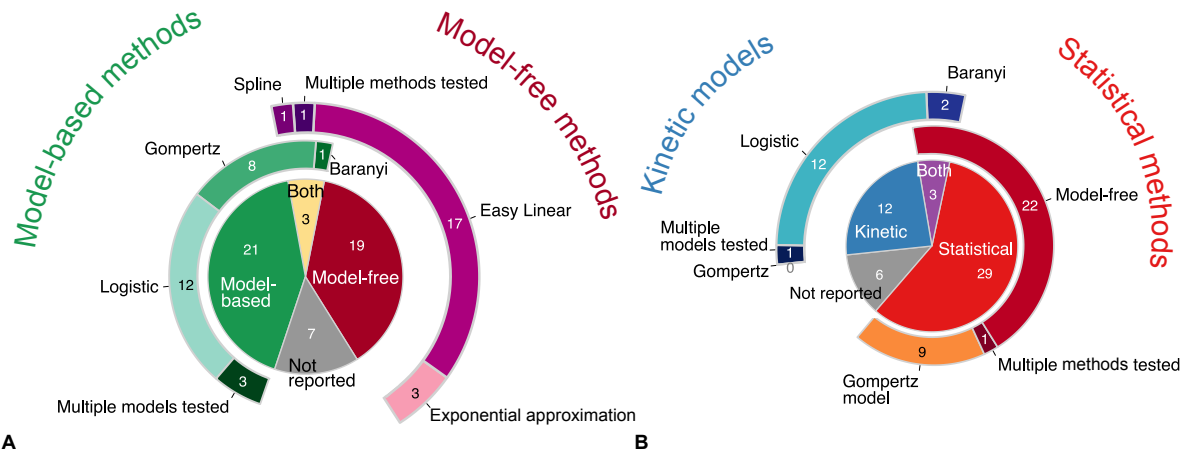


Figure 2: Pie and doughnut charts of literature review results. **A) Model-free methods were used about as often as model-based methods** across all 50 papers reviewed. “Both” refers to when both a model-free and a model-based method were used in the same paper. The doughnut charts surrounding the central pie-chart illustrate how frequently different models, including both statistical and kinetic models, were used (left, shades of green) and how frequently different statistical model-free methods were used (right, shades of purple). **B) Statistical approaches were used more often than kinetic models.** “Both” refers to when both a kinetic model(s) and a statistical approach(es) were used in the same paper. The doughnut charts surrounding the central pie-chart illustrate how frequently different kinetic models were used (left, shades of blue) and how frequently different statistical approaches were used (right, shades of red-orange). The Gompertz model is listed twice because it is either a kinetic model or a statistical model, depending on the equation; however, no paper was found to use a kinetic Gompertz model. Both of the statistical Gompertz models listed in Table 1, Gompertz and modified Gompertz, are grouped together. For more details on the methods and equations used by each paper, see table S1. All slices within each pie and doughnut chart show the counts of papers included.

166 2.2 Exposition of existing models and methods

167 2.2.1 Conceptual distinctions between parametric vs non-parametric methods 168 and statistical vs kinetic models

169 A variety of approaches have been developed over the years to describe and quantify growth
170 curves, as shown in Figure 2. Below we explain the main differences between the most
171 commonly used approaches and models, then we compare the advantages of each.

172 **Model-free vs model-based methods:**

173 One way to classify the different methods is to distinguish between model-free (or non-
174 parametric) methods and model-based (or parametric) methods. Model-free methods use
175 an algorithm to find an estimate of the growth rate that is relatively robust to any noise error
176 in the data. For example, in the classical exponential approximation from Monod (1949)
177 that is featured in many introductory microbiology textbooks, growth rate is estimated by
178 measuring cell concentrations (N_1 and N_2) at two time points (t_1 and t_2) during the “log”
179 phase of growth, then calculating $R = (\log_2 N_2 - \log_2 N_1)/(t_2 - t_1)$. This is an algorithm
180 that can easily be used by hand or performed by a computer. The Easy Linear method (Hall
181 et al., 2014; Mira et al., 2017) is a more complex algorithm that uses a sliding window of five
182 successive data points to calculate the maximum slope among many linear regressions fitted
183 to the log-scale growth curve data. Another example is the Spline method that calculates the
184 maximum value of the first derivative of the log-scale growth curve data by either using the
185 mean of three successive pairs of points (e.g., Ashino et al. 2019) or kernel smoothing of the
186 growth curve (e.g., Kahm et al. 2010; Petzoldt 2020) in order to remove experimental noise.
187 The parameters of these algorithms are usually tunable, for example the size of the sliding
188 window used by the Easy Linear method. However, no explicit assumptions are made about
189 the shape of the growth curves.

190 Model-based methods, on the other hand, use equations to explicitly describe the relation-
191 ship between time, the independent variable, and population size (or a proxy of population
192 size, like OD), the dependent variable. A model fitting algorithm is then used to find the
193 model parameters that best fit the observed data, usually by numerical minimization of the
194 residual sum of squares. Model-based methods tend to be preferred by theoretical and sta-
195 tistical biologists because models specifically define the assumptions that are being made,
196 model-based methods have defined protocols for assessing goodness of fit, and model-fitting
197 allows quantification of the (frequentist or Bayesian) error of the estimates (Otto and Day,
198 2011; Bolker, 2008).

199 Empiricists tend to prefer to apply model-free approaches to biological growth curve data
200 both because it is technically more difficult to fit and compare models and because of the
201 inflexibility of existing models to fit the data (source: personal communication). In other
202 words, the main advantage of model-free approaches is that they do not require a model.
203 Model-free approaches have drawbacks, however: since there is no model, it is not clear how
204 to compare the likelihood or goodness-of-fit between different methods and bootstrapping is
205 necessary to quantify the error around estimates (for example, in order to generate the 95%
206 confidence intervals).

207 **Kinetic vs statistical models:**

208 Within model-based methods, there is a distinction between kinetic and statistical models.
209 Kinetic models may also be called mechanistic/process models and statistical models can be
210 called phenomenological/pattern models (Bolker, 2008). We define kinetic models as mecha-

211 nistic representations that simulate the underlying process of interest. For population growth
212 curve models in particular, the *per capita* growth rate of a kinetic model is by definition the
213 intrinsic growth rate μ when the cell's resources are limitless or otherwise optimal.

214 Statistical models can be thought of as 'black-box empirical models' (Chezeau and Vial,
215 2019). They are created by selecting functions that have a similar shape as the pattern of
216 interest. Then, the parameters of those functions are given a biologically relevant meaning.
217 For growth curves in particular, statistical population growth models are defined such that
218 the point on the curve with the fastest rate of *per capita* growth (i.e., the inflection point
219 of $y = \ln(N/N_0)$) corresponds to the maximum growth rate μ_{\max} (Zwietering et al., 1990,
220 equations 4 & 5). Model-free (non-parameteric) methods all belong to the statistical category,
221 as shown in Figure 2B, as they quantify specific parameters of interest without simulating the
222 underlying process.

223 Although the distinction between kinetic models and statistical methods may seem arcane,
224 we explain below how serious pitfalls in estimating growth rates are a direct result of the
225 differences between growth rates estimated by kinetic models (i.e., the intrinsic growth rate
226 μ) and statistical methods (i.e., the maximum growth rate μ_{\max}).

227 **2.2.2 Mathematical description of models and model parameters, including the** 228 **initial fraction**

229 Many models have been developed to describe growth curves (e.g., Tsoularis and Wallace 2002;
230 Huang 2011; Baranyi and Roberts 1994). We have summarized the equations and parameters
231 of the most prevalent models found by our literature review in Table 1, distinguishing kinetic
232 models (Kin) from statistical models (S). As explained in the section above, a main difference
233 to note is that kinetic models are defined in terms of the intrinsic growth rate μ , whereas
234 statistical models are defined in terms of the maximum growth rate μ_{\max} . Kinetic models
235 describe population size N as a function of time (i.e., linear scale), whereas statistical models
236 describe $y = \ln(N/N_0)$ as a function of time (i.e., they operate on a logarithmic scale).

237 The common feature of all models, whether kinetic or statistical, is that they have a
238 sigmoid or 'S' shape (Zwietering et al., 1990). All models consider single-strain, well-mixed
239 bacterial populations whose every individual divides at the same *per capita* rate, although the
240 division rate varies over time. Each of these populations starts with N_0 microbes and their
241 maximum population size is defined by a carrying capacity, written as K for kinetic models
242 or A for statistical models.

243 The models differ in important ways. Most of the models derive from the logistic model
244 but seek to generalize it (Tsoularis and Wallace, 2002). For example, the Richards (both
245 kinetic and statistical) and Baranyi models include a parameter to set the growth inflection
246 and a lag phase, respectively, whereas the Huang model incorporates both. The Gompertz
247 models (both kinetic and statistical) have no additional parameters but display faster growth
248 than the logistic model for the same set of parameters since they have a higher *per capita*
249 growth rate. Furthermore, the Richards model requires an extra parameter β that determines
250 how quickly deceleration occurs as the stationary phase is reached, whereas the Baranyi model
251 includes a lag phase specified by the parameter h_0 . The Huang model includes a lag phase
252 defined by τ in addition to a parameter α determining the curvature.

253 The initial fraction, N_0/K , is an important value to keep in mind throughout our paper.
254 This is the size of the population at inoculation (i.e., N at time $t = 0$) divided by the final

255 carrying capacity. Only when the initial fraction is small can one distinguish models that
256 have an initial exponential growth, like the logistic model, from models with a lag phase, like
257 the Gompertz, Richards, Baranyi, and Huang models.

258 **2.2.3 What is the difference between μ and μ_{\max} ?**

259 It is important to distinguish between three growth rate estimators: the maximum population
260 growth rate ($\max(dN/dt)$), the *per capita* maximum growth rate (μ_{\max}), and the *per capita*
261 intrinsic growth rate (μ). The maximum population growth rate $\max(dN/dt)$ is the fastest
262 increase in size achieved by the *entire population*. We are not interested in the maximum
263 population growth rate parameter since it is not estimated by any of the methods or models we
264 discuss here; we only mention it so that the reader does not mistake it for the maximum growth
265 rate (μ_{\max}). The maximum growth rate μ_{\max} is the fastest *per capita* number of divisions
266 per unit of time actually achieved in the observed growth curve. In more quantitative terms,
267 μ_{\max} is the maximum value of the curve $d \ln(N/N_0)/dt$ (Figures 1B-C). As mentioned above,
268 the maximum growth rate μ_{\max} is a value estimated using statistical approaches. Finally, the
269 intrinsic growth rate μ (sometimes denoted as r (Sprouffske and Wagner, 2016), called the
270 Malthusian parameter of population growth, or the intrinsic rate of increase) is the fastest *per*
271 *capita* number of divisions per unit of time theoretically possible and, because it is a kinetic
272 model parameter, it is used for simulating population growth processes. We here focus on
273 the intrinsic growth rate μ and the maximum growth rate μ_{\max} because these are the two
274 quantities estimated by the most used methods.

275 There is an important conceptual difference between the intrinsic growth rate μ and the
276 maximum growth rate μ_{\max} . The intrinsic growth rate μ is the theoretical maximum number
277 of cell divisions per time unit assuming population dynamics that follow an exponential law.
278 However, No real population achieves an infinite size because the division process is limited
279 by space and/or nutrients, for instance. Thus, the number of divisions per time unit is
280 not constant over time, so the maximum division rate μ_{\max} is the largest *per capita* value
281 observed during the population growth. Therefore, the intrinsic growth rate μ can quantify
282 the strain-specific division rate theoretically independently of the environment or experimental
283 conditions. On the other hand, the maximum growth rate μ_{\max} (like other values estimated
284 by statistical methods) is always specific to the experiment itself and cannot be generalized
285 as a strain-specific value that applies to different environments or conditions. As will be
286 shown below, in the best case scenario μ_{\max} approximates μ , but in other scenarios μ_{\max} is a
287 composite parameter that depends on other values, like the inoculum size and lag time.

288 Previous work has pointed out confusions between different growth rate estimators (Perni
289 et al., 2005). The confusion between these terms is so prevalent that some papers mistook μ
290 for μ_{\max} (Yang et al., 2006), vice versa (Wu et al., 2017), or distinguished between the two but
291 swapped the names (Khan et al., 2017). Furthermore, some authors wrote the kinetic logistic
292 equation as $dN/dt = \mu_{\max}(1 - N_0/K)N$ (Petzoldt, 2020), whereas other authors preferred
293 $dN/dt = \mu(1 - N/K)N$ and $\mu_{\max} = \max(d \ln(N(t)/N_0)/dt)$ (Sprouffske and Wagner, 2016).
294 Different naming conventions become even more misleading for models in which the intrinsic
295 growth rate is a function of the resource concentration, such as the Monod class of models that
296 have their own specific, kinetic definition for μ_{max} (Monod, 1949; Chezeau and Vial, 2019).
297 We will not discuss substrate-use models herein. Having explained the conceptual differences
298 between the μ_{\max} maximum growth and μ intrinsic growth rates above, we now expand on

Model	Equation	Parameters
Logistic (Kin)	$N(t) = \frac{N_0 K \exp(\mu t)}{K + N_0 (\exp(\mu t) - 1)}$	K, N_0, μ
Gompertz (Kin)	$N(t) = (N_0/K) \exp(-\mu t) K$	K, N_0, μ
Richards (Kin)	$N(t) = \frac{N_0 K}{(N_0^\beta + (K^\beta - N_0^\beta) \exp(-\mu \beta t))^{-1/\beta}}$	K, N_0, μ, β
Baranyi (Kin)	$N(t) = \frac{(-1 + \exp(h_0) + \exp(\mu t)) N_0 K}{(\exp(\mu t) - 1) N_0 + \exp(h_0) K}$	K, N_0, μ, h_0
Huang (Kin)	$N(t) = \frac{N_0 K}{N_0 + (K - N_0) (1 + \exp(\alpha \tau))^{\mu/\alpha} (\exp(\alpha t) + \exp(\alpha \tau))^{-\mu/\alpha}}$	$K, N_0, \mu, \alpha, \tau$
Logistic (S)	$y(t) = \frac{A}{1 + \exp(4\mu_{\max}(\lambda - t)/A + 2)}$	A, μ_{\max}, λ
Gompertz (S)	$y(t) = A \exp(-\exp(\mu_{\max} \exp(1)(\lambda - t)/A + 1))$	A, μ_{\max}, λ
modified Gompertz (S)	$y(t) = A \exp(-\exp(\mu_{\max} \exp(1)(\lambda - t)/A + 1)) + A \exp(\alpha(t - t_{shift}))$	$A, \mu_{\max}, \lambda, \alpha, t_{shift}$
Richards (S)	$y(t) = A(1 + \nu \exp(1 + \nu + \mu_{\max}(1 + \nu)^{1+1/\nu}(\lambda - t)/A))^{-1/\nu}$	$A, \mu_{\max}, \lambda, \nu$

Table 1: Different population growth models: The population growth models considered in this paper with their equation and parameters. Kinetic models are indicated by (Kin) and describe the population size N as a function of time t . Every kinetic model includes a carrying capacity K , an initial population size N_0 and an intrinsic growth rate μ . The kinetic Richards model includes a parameter β to adjust its inflection point and the Baranyi model has a lag phase defined by h_0 . The Huang model has both with parameters α and τ , respectively. Statistical models are indicated by (S) and describe $y = \ln(N/N_0)$ as a function of time t . Every statistical model includes a carrying capacity $A = \ln(K/N_0)$, a maximum growth rate μ_{\max} and a lag phase λ . The modified Gompertz model (S) displays a second increase after the growth reaches a first saturation plateau. The parameters t_{shift} and α control the time and the slope of the second increase. The inflection point in the statistical Richards model is adjustable by the parameter ν .

299 the mathematical differences.

300 **Deriving the difference between μ_{\max} vs. μ :**

301 In the following, we mathematically explain why μ_{\max} is not always a good proxy for μ ,
302 especially at large initial population fractions, N_0/K . Analytical math is combined with
303 simulations to show for which initial population fractions an experimenter can estimate the
304 intrinsic growth rate μ from the maximum growth rate μ_{\max} .

305 We assumed that the population dynamics follow one of the kinetic growth models from
306 Table 1 and mathematically derived μ_{\max} for the five kinetic models. As reported in Table 2,
307 μ_{\max} depends on the system parameters, namely the initial population fraction N_0/K as well
308 as the parameters β and h_0 for the Richards and the Baranyi models, respectively.

309 The results of Table 2 are illustrated by the points in Figure 3A. The estimated maximum
310 growth rate (μ_{\max}) values differ between models with the same parameter values (intrinsic
311 growth rate $\mu = 1$ and carrying capacity $K = 10^5$). In general, the maximum growth rate
312 is approximately equal to the intrinsic growth rate when the initial fraction of individuals
313 satisfies $N_0/K \ll 1$ and $(N_0/K)^\beta \ll 1$ in the Logistic and Richards models, respectively.
314 Indeed, these conditions lead to $\mu_{\max} = \mu(1 - N_0/K) \approx \mu$ and $\mu_{\max} = \mu(1 - (N_0/K)^\beta) \approx \mu$
315 for the Logistic and Richards models, respectively (see Table 2). The Gompertz model is a
316 special case since the maximum division rate is a good proxy for the intrinsic division rate
317 when the initial fraction is large, roughly equal to $\exp(-1) \approx 0.37$ (i.e., an inoculum size
318 corresponding to a dilution factor for the stationary phase batch culture of between one-third
319 and two-fifths).

320 In order to test the analytical predictions from Table 2, we evaluated the growth rates
321 as estimated by model-free methods using data simulated under each of the five population
322 growth models. Unlike experimental data, for which the true μ value that generated the
323 data is never known, estimating the growth rate from simulated data allows us to check the
324 accuracy of the estimates as compared to the known μ parameter that the data was simulated
325 under.

326 We focus on two model-free methods, the popular Easy Linear (Hall et al., 2014) and
327 the Spline (e.g., Adkar et al. 2017; Ashino et al. 2019) methods, to determine the maximum
328 growth rate μ_{\max} . Both methods assume that only the exponential stage of growth is useful to
329 estimate the maximum growth rate. We generated data using individual based stochastic sim-
330 ulations for the Gompertz, Richards, Logistic, Huang, and Baranyi models. Then we used the
331 two different model-free methods, Spline and Easy Linear, to compute the maximum growth
332 rate μ_{\max} for different parameter values. In practice, both model-free methods provided us
333 with the same results. Our simulated data averaged over several stochastic realizations did
334 not include the myriad sources of noise present in experiments, therefore resulting in a low
335 noise level.

336 As shown by the lines in Figure 3A, there is an excellent agreement between our analytical
337 predictions (lines) and the estimates from simulated data (points). As predicted analytically,
338 the estimated maximum growth rate μ_{\max} is not equal to the known intrinsic growth rate μ
339 value used to create the simulations, unless $N_0/K \ll 1$. For the Baranyi, Huang, Logistic, and
340 Richards models, the smaller the initial population fraction, the better the maximum growth
341 rate performs as a proxy for estimating the intrinsic bacterial growth rate, μ . However, this is
342 not the case for the Gompertz model. For the Baranyi and Richards models (supplementary
343 Figures S4A and S4B), the smaller the parameter h_0 and the larger the parameter β , the
344 closer is the maximum growth rate μ_{\max} to the intrinsic growth rate μ . Similarly, for the

Model	Derived maximum growth rate μ_{\max}
Logistic (Kin)	$\mu(1 - N_0/K)$
Gompertz (Kin)	$-\mu \ln(N_0/K)$
Richards (Kin)	$\mu(1 - (N_0/K)^\beta)$
Baranyi (Kin)	$\frac{\mu e^{-h_0} (-2(1 + \sqrt{(-1 + e^{h_0})(e^{h_0}(K/N_0) - 1)})(N_0/K) + e^{h_0}(1 + N_0/K))}{1 - N_0/K}$
Huang (Kin)	Numerical solution
Logistic (S)	μ_{\max}
Gompertz (S)	μ_{\max}
modified Gompertz (S)	μ_{\max}
Richards (S)	μ_{\max}

Table 2: **Maximum growth rates:** The maximum growth rate μ_{\max} for the population growth models considered in this paper. Kinetic models are indicated by (Kin), whereas the statistical models are indicated by (S). The maximum growth rate was derived for the kinetic models by analytically determining $\max(dy/dt) = \max(d \ln(N/N_0)/dt)$. All statistical models have the same maximum growth rate, whereas the maximum growth rate differs between kinetic models.

345 Huang model, the higher the curvature defined by α and the shorter the duration τ of the lag
 346 phase, the better μ_{\max} is as a proxy for μ (see Figures S4C and S4D).

347 We have shown that the maximum growth rate μ_{\max} is not always equivalent to the
 348 intrinsic growth rate μ . Therefore, methods that estimate the maximum growth rate μ_{\max}
 349 but then (often implicitly) assume that this value can be treated as the μ of a kinetic model
 350 must be applied with caution. As we have demonstrated in Table 2 and Figure 3A, μ_{\max}
 351 tends to *underestimate* the true intrinsic growth rate μ – except when population growth
 352 follows the Gompertz kinetic model, in which case the maximum growth rate μ_{\max} mostly
 353 *overestimate* the true intrinsic growth rate μ . This is because the *per capita* growth rate is
 354 generally smaller than the intrinsic one. Hence, we recommend that a clear distinction must
 355 be made between the intrinsic growth rate μ and the maximum growth rate μ_{\max} .

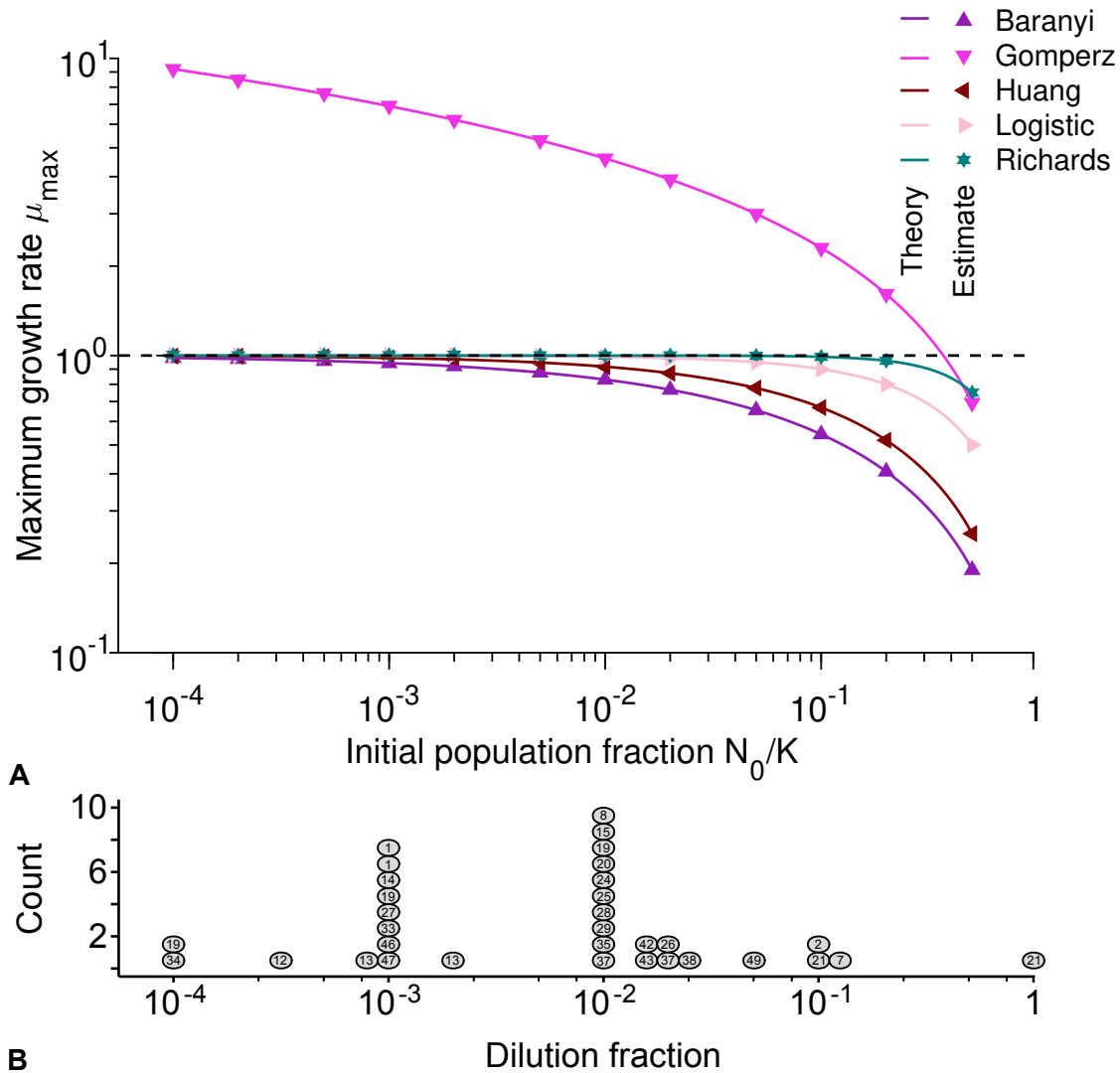


Figure 3: **A) The Gompertz model and large initial population fractions make the maximum growth rate a poor proxy for the intrinsic growth rate:** Maximum growth rate μ_{\max} versus initial population fraction N_0/K for different kinetic population growth models, where $\mu = 1$. Each point represents estimated values by Spline (from Petzoldt 2020) from simulated data averaged over 10^4 stochastic realizations. The solid lines correspond to the analytical predictions of the maximum growth rate (see Table 2). The dashed line shows the intrinsic growth rate value μ . Parameter values: $K = 10^5$, $\mu = 1$, $\alpha = 2$, $\beta = 2$, $h_0 = 2$ and $\tau = 2$. The initial population fraction is defined as a combination of model parameters, N_0/K , while the initial dilution fraction is an empirical quantity extracted from experimental data as detailed in the literature review methods. **B) For the most commonly used dilution fractions in the literature, the maximum growth rate is a good proxy for the intrinsic growth rate:** Histogram of the estimated dilution fractions observed for the 27 (out of 50) papers that provided sufficient information to estimate this value. Each circle represents a publication and the number inside the circle indicates the number of the reference as given in supplementary table S1. Several publications appear more than once because they used more than one dilution fraction for different experiments.

356 **The initial fraction is a key parameter determining the relationship of μ_{\max}**
357 **and μ**

358 Above we showed that (for most models) we can use the estimated maximum growth rate
359 μ_{\max} as an approximation of μ when initial population fractions N_0/K are small. We esti-
360 mated the initial dilution fractions used in different experiments in order to ascertain whether
361 most studies are using appropriately small initial fractions. Figure 3B shows the estimated
362 dilution fractions used by different papers included in our literature review. Papers that had
363 experiments with multiple, different batch culture starting conditions are included as multi-
364 ple points with the same number. For example, Ganucci et al. 2018 (labeled as 21) has a
365 dilution fraction near 1. The authors used cell viability counts to track yeast growth in media
366 with increasing ethanol concentrations, sometimes resulting in almost no growth. Two values
367 from Ganucci et al. (2018) are summarized in Figure 3B, indicating the largest (0.1) and the
368 smallest (0.94) dilution fractions observed. Since methods differ between publications, with
369 some using a mid-exponential phase culture and others using a stationary phase culture for
370 inoculation (see supplementary table S1), the estimated dilution fraction should be considered
371 as an upper bound for the initial fraction used in each paper.

372 More than two-thirds of papers use at least one estimated dilution fraction smaller than
373 10^{-2} ; the geometric-mean observed dilution fraction was $10^{-2.7}$. For such small dilution
374 fractions, if there is no lag time, and if growth follows one of the population growth models
375 except Gompertz, the maximum growth rate μ_{\max} tends to be a good estimator of the intrinsic
376 growth rate μ . When the true growth curve dynamics in the experiments follows one of the
377 kinetic models other than Gompertz, the relative difference between the maximum growth
378 rate and the intrinsic growth rate for the mean initial population fraction $N_0/K = 10^{-2.7}$ is
379 between 0-12%. Here, the largest difference between μ_{\max} and μ is obtained for the Baranyi
380 model. However, for the Gompertz model the relative difference between the maximum growth
381 rate and the intrinsic growth ranges from -821% to 31% (see Figure 3).

382 **Discussion of the difference between μ_{\max} and μ :**

383 We showed that the μ_{\max} values calculated from kinetic models depend on other parameters
384 in addition to μ , such as the initial population fraction. Conversely, one cannot obtain μ
385 from μ_{\max} alone. For kinetic models, additional parameters such as the initial population
386 size and carrying capacity are required (see Table 1) to be able to calculate μ from μ_{\max} .
387 For statistical approaches, which are specified directly in terms of μ_{\max} , μ is not defined.
388 Nevertheless, even when μ_{\max} is estimated by statistical models, its estimated value will
389 be different when experimental quantities such as the initial population size and carrying
390 capacity change. In reality, the estimated values for both μ_{\max} and μ may also vary with the
391 experimental conditions (such as genotype, medium, temperature, etc).

392 We emphasize that the main difference between the maximum growth rate μ_{\max} and the
393 intrinsic growth rate μ is that μ_{\max} is a statistical quantity, whereas μ is a model parameter.
394 Therefore, obtaining different estimates of μ and μ_{\max} is expected and not a sign of bad
395 performance of a model or method, especially for large initial population fractions. For
396 example, the manual of one software (Delaney, 2014) provides options for fitting various
397 statistical models and a single kinetic model but discourages users from applying the kinetic
398 model because “it predicts fastest growth” as compared to the other implemented models.
399 Our results can readily explain this observation and debunk the implied worse performance of
400 the kinetic model. Indeed, the publication associated with this software recommends a large
401 inoculum size (Delaney et al. 2013; associated studies labeled as 8, 22, 25, 42, and 43 in Figure

402 3B and supplementary table S1), for which we showed that μ_{\max} consistently overestimates
403 μ .

404 Given the differences between μ_{\max} and μ , which of these should preferably be estimated?
405 Unfortunately, there is not a one-size-fits-all answer to this question. From a theoretician’s
406 perspective, we recommend that researchers estimate the intrinsic growth rate μ . Most studies
407 perform growth curve experiments to characterize growth for specific strains, treatments, or
408 environments in the (either explicit or implicit) context of population ecology or mechanistic
409 models – all of which are defined in terms of μ . Only the intrinsic growth rate μ can be
410 used for simulating mechanistic models and therefore to identify the mechanisms which best
411 explain the observed dynamics. The maximum growth rate μ_{\max} , on the other hand, is phe-
412 nomenological: it describes what is observed in the data contingent on the population starting
413 conditions and the experimental environment. At best, μ_{\max} approximates μ . However, from
414 an experimenter’s perspective, estimating μ_{\max} has the advantage that model-free methods
415 are technically easier to use than estimators of kinetic models, especially for data that dis-
416 play diphasic or other non-sigmoid/non-‘S’ shaped growth. We strongly urge researchers who
417 decide to estimate μ_{\max} to use (and report) a small initial population fraction and to assert
418 that the data do not have a significant lag time.

419 When using statistical methods, a second decision is necessary about whether to use model-
420 based or model-free methods. In our noise-free, simulated data, model-based and model-free
421 statistical methods yielded the same estimates for μ_{\max} (Figure 3A); future work should
422 elaborate on their performance in the presence of different sources of noise (e.g., to expand
423 on the work that has already been done by Mira et al. (2017) for the Easy Linear method).
424 Although models are preferable from a theoretician’s view, certain types of experimental data
425 (for example, displaying diauxic growth, curves without samples in the stationary phase, and
426 other non-sigmoid shaped data as well as very noisy data) may not be fitted well by a model of
427 sigmoidal growth. In this case the data may be better summarized by a model-free statistical
428 method. Importantly, we recommend that the choice of method is justified clearly and in
429 writing, no matter which method is used.

430 2.3 Guidelines for estimating growth rates

431 2.3.1 Ad hoc fitting an exponential curve to growth curves should be avoided

432 One common approximation (Monod, 1949; Kassen, 2014) that is used to obtain an estimate
433 of the intrinsic growth rate μ is to fit an exponential equation, like $N(t) = N_0 e^{\mu t}$, to the early
434 phases of growth (i.e., during the “log”/“linear” phase, prior to the deceleration and stationary
435 phases). This method is explained in many introductory microbiology textbooks, as previously
436 summarized in the explanation of model-free methods of section 2.2.1 above, and we refer to
437 this approach as an exponential approximation. Under the exponential approximation, the
438 intrinsic growth rate is given by $\mu = \ln(N(t)/N_0)/t$.

439 To test the accuracy of the exponential approximation when applied to batch culture
440 population growth, we expressed the intrinsic growth rate as a function of population size
441 and other possible parameters for different kinetic population growth models (Table 3 and
442 Figure S5).

443 We found that the exponential approximation is frequently a poor estimator of the intrinsic
444 growth rate μ . The exponential approach is never valid for a population following Gompertz

Kinetic model	Intrinsic growth rate μ
Exponential	$\ln \left(\frac{N(t)}{N_0} \right) / t$
Logistic	$\ln \left(\frac{N(t)}{N_0} \frac{1-N_0/K}{1-N(t)/K} \right) / t$
Gompertz	$\ln \left(\frac{\ln(N_0/K)}{\ln(N(t)/K)} \right) / t$
Richards	$\ln \left(\frac{(N(t)/N_0)^\beta (1-(N_0/K)^\beta)}{1-(N(t)/K)^\beta} \right) / (t\beta)$
Baranyi	$\ln \left(1 - \frac{e^{h_0(1-N(t)/N_0)}}{1-N(t)/K} \right) / t$
Huang	$\alpha \frac{\ln((-1+K/N(t))/(1-K/N_0))}{\ln((1+e^{\alpha\tau})/(e^{\alpha t}-e^{\alpha\tau}))}$

Table 3: **Intrinsic growth rate as function of the model parameters at time t for different kinetic population growth models** The difference between the equations indicates that the exponential approximation may often not be appropriate; see also Figure S5.

445 growth. There is no parameter range for which the equation $\ln(\ln(N_0/K)/\ln(N(t)/K))/t$
 446 reduces to $\ln(N(t)/N_0)/t$ (see Table 3). The exponential approach is valid for the lo-
 447 gistic growth when the initial population size is very small in comparison to the carry-
 448 ing capacity (i.e., $N_0 \ll K$) and for time points at which the population size remains
 449 small in comparison to the carrying capacity (i.e., $N(t) \ll K$). These conditions lead to
 450 $\ln(N(t)(1 - N_0/K)/(N_0(1 - N(t)/K)))/t \approx \ln(N(t)/N_0)/t$ (see Table 3). This makes sense
 451 since the phase during which these conditions are satisfied corresponds to the regime in
 452 which logistic growth can be reduced to exponential growth. The same conditions apply
 453 to Baranyi growth, with the additional condition that the lag phase must be short (i.e.,
 454 $h_0 \ll 1$), so that one obtains $\ln(1 - e^{h_0(1 - N(t)/N_0)}/(1 - N(t)/K))/t \approx \ln(N(t)/N_0)/t$
 455 (see Table 3). If the lag phase is not short, the exponential phase starts later whereas the
 456 exponential approach assumes that it starts at the beginning of the growth. Richards growth
 457 is more complex. Here, the quantities $(N_0/K)^\beta$ and $(N(t)/K)^\beta$ must be much less than 1
 458 to make the exponential approach valid. Thus, the larger the deceleration parameter β is
 459 when $N_0 \ll K$ and $N \ll K$, the more abruptly the “log”/“linear” phase transitions into
 460 the stationary phase, and the more valid the exponential approximation becomes, so that
 461 $\ln((N(t)/N_0)^\beta(1 - (N_0/K)^\beta)/(1 - (N(t)/K)^\beta))/t \approx \ln(N(t)/N_0)/t$ (see Table 3). Con-
 462 sequently, the exponential approximation is valid only in a very restricted set of conditions:
 463 when there is no lag phase, the initial population fraction is very small, and the measured
 464 population sizes remain small as compared to the carrying capacity. Most experimental data
 465 probably do not meet this necessary set of conditions.

466 It is of note that throughout the literature, including introductory textbooks, the term
 467 “exponential growth rate” tends to be used to describe the intrinsic growth rate μ and some-

468 times deemed the same as the maximum growth rate μ_{\max} (e.g., Basra et al. 2018; Novak
469 et al. 2009). We here strongly caution against this conflation of potentially very different
470 quantities. In particular, we recommend that approximating batch culture growth with an
471 exponential curve in order to get an estimate for the intrinsic growth rate μ requires careful
472 assurance that the assumption is valid for the data at hand.

473 **2.3.2 Theory predicts that using μ_{\max} or the exponential approximation for es-** 474 **timating relative fitness can yield wrong results**

475 In evolution and population biology, the relative fitness w of a mutant (M) compared to a
476 wild-type (WT) is classically defined as the ratio of μ^M/μ^{WT} . The relative fitness or the
477 selection coefficient, defined as $s \equiv w - 1 = \mu^M/\mu^{WT} - 1$, is used to classify a mutant as
478 deleterious ($w < 1$ or $s < 0$), neutral ($w = 1$ or $s = 0$), or beneficial ($w > 1$ or $s > 0$).
479 Thus, to infer how natural selection favors one strain over another from monoculture growth
480 curves, microbial ecologists and evolutionary biologists need the intrinsic growth rate, which
481 is obtained by fitting a kinetic model.

482 One argument regarding the issues of miscalculation of the intrinsic growth rate μ discussed
483 above is that these concerns are important for *absolute* growth rate estimates, but can be
484 disregarded when considering *relative* estimates. Here, the argument is that whereas absolute
485 estimates cannot be compared between data-sets, relative growth rates can be estimated
486 within a data-set by using a common reference sample and these relative growth rates can then
487 be compared between data-sets. Moreover, with regards to selection coefficients, the sign may
488 be more important than the absolute value. Namely, incorrect absolute estimates should yield
489 correct rankings of growth rate estimates, and thus correctly estimated signs of the selection
490 coefficient. Below, we demonstrate that these assumptions are wrong and that incorrect
491 estimates of the growth rates (for example, by assuming that $\mu_{\max} = \mu$) can severely affect
492 the classification of strains into beneficial, neutral, or deleterious.

493 To demonstrate the effects on relative fitness estimates of assuming $\mu_{\max} = \mu$, we simulated
494 growth curve data from separate batch monocultures for two strains and estimated their
495 maximum growth rates μ_{\max} using the growth curves. Then we assumed (erronously) that
496 the maximum growth rate μ_{\max} was a good approximation of the intrinsic growth rate μ . We
497 calculated the relative fitness of the mutant with respect to the wild-type as $w = \mu_{\max}^M/\mu_{\max}^{WT}$
498 (or the selection coefficient as $s = \mu_{\max}^M/\mu_{\max}^{WT} - 1$).

499 Figure 4A shows that using μ_{\max} to estimate the relative fitness generally infers incorrect
500 values for the relative fitness (as well as the selection coefficient), unless both strains have
501 exactly the same initial population fraction (N_0/K). Even more concerning, this estimation
502 sometimes categorizes the mutant as deleterious when it is beneficial, and vice versa. This
503 is especially worrisome because we assumed noise-free data and an ideal case in which both
504 bacterial strains follow the same population dynamics. In summary, equivocating μ_{\max} with
505 μ is likely to lead to wrong estimates of fitness and selection coefficients.

506 Mis-estimation of the selection coefficient also occurs when calculating relative growth rate
507 values using the exponential approximation. Lenski et al. (1991) extended the exponential
508 approximation to calculate the fitness of a mutant strain (M) relative to the fitness of a
509 wild-type strain (WT), $w = \ln(N^M(t)/N_0^M)/\ln(N^{WT}(t)/N_0^{WT})$ (or the selection coefficient
510 $s \equiv w - 1 = \ln(N^M(t)/N_0^M)/\ln(N^{WT}(t)/N_0^{WT}) - 1$). Note that under the assumption of
511 exponential growth, both the relative fitness and the selection coefficient measured by the

512 equation stated above are time-independent. Both Lenski et al. (1991) and Ram et al. (2019)
513 empirically set the time interval of measurements t to 24 hours.

514 Similarly to using μ_{\max} as a proxy for μ , the exponential approximation yields wrong es-
515 timates for the relative fitness (as well as the selection coefficient) in many cases (Figure 4B).
516 For growth curves (except for the Gompertz model) in which the initial population fraction
517 of the mutant is smaller than that of the wild-type, the exponential approximation is a more
518 conservative estimator than μ_{\max} ; it is less likely to overestimate the relative fitness. However,
519 when the initial population fraction of the mutant is larger than that of the wild-type, the
520 exponential approximation is likely to incorrectly infer that a beneficial mutant is deleteri-
521 ous (Figure 4B). Thus, the exponential approximation both misestimates and misclassifies
522 throughout much of the experimentally reasonable parameter range.

523 **Implications for the estimation of selection coefficients from growth rates:**

524 We showed that using μ_{\max} as a proxy for μ in order to calculate the relative growth rates or
525 relative fitness can lead to biased estimates (Figure 4). The amount of bias in the estimate
526 becomes larger as the difference in the true growth parameters between the two studied strains
527 becomes larger. Accordingly, we strongly recommend that experimenters use the intrinsic
528 growth rate μ to estimate relative fitness. According to population biology, relative fitness
529 is defined as the ratio of the intrinsic growth rate of the mutant strain over the wild-type
530 strain, μ^M/μ^{WT} (Lenski et al., 1991; Crow and Kimura, 2009; Chevin, 2011). From this
531 point of view, it follows that relative fitness can only be estimated using the intrinsic growth
532 rate μ . Nevertheless, fitness-related phenotypes, like $\mu_{\max}^M/\mu_{\max}^{WT}$, are sometimes used as a
533 summary statistic of population growth that is contextual to the environmental, temporal,
534 and population conditions (e.g., Adkar et al. 2017). Above we showed that a proxy of the
535 intrinsic growth rate (like μ_{\max} or the exponential approximation) can accurately estimate
536 the relative fitness only if specific criteria are met. When these criteria are *not* met, μ_{\max}
537 becomes a composite parameter that depends on other experimental quantities that should
538 be reported, like the initial fraction and lag time. Only if experiments are set up with small
539 and equal initial fractions of the mutant and wild-type strains and if the strains do not exhibit
540 a lag phase, using μ_{\max} as a proxy for μ to estimate the relative fitness may be justified.

541 **2.4 Application of theory: Re-analyzing 4 published data-sets**

542 In order to clarify the theoretical considerations discussed above, we re-analyzed four pub-
543 lished data-sets using the diversity of methods discussed above and then compared how the
544 different methods performed on the same data. Among the 50 studies reviewed, we identified
545 four that were appropriate for re-analysis since these papers provided their complete data-set
546 and reported their estimated values (Adkar et al., 2017; Hammer et al., 2021; Ram et al.,
547 2019; Todd and Selmecki, 2020). Each of these bacterial growth curve data-sets reports op-
548 tical density versus time for different bacterial strains, with a total of 142 curves across all
549 studies. We used three publicly available R packages, Growthcurver, grofit and growthrates,
550 to estimate growth parameters (Sprouffske and Wagner, 2016; Kahm et al., 2010; Petzoldt,
551 2020). We tested two model-free methods (Spline and Easy Linear) and the model-based
552 methods listed in Table 1. These models are based on different equations that are statistical
553 (Zwietering et al., 1990) or kinetic (Tsoularis and Wallace, 2002; Baranyi and Roberts, 1994;
554 Huang, 2011). We focused on inferring the maximum growth rate (μ_{\max}), both because it is
555 of greatest relevance to the work discussed above and because it is the only quantity common

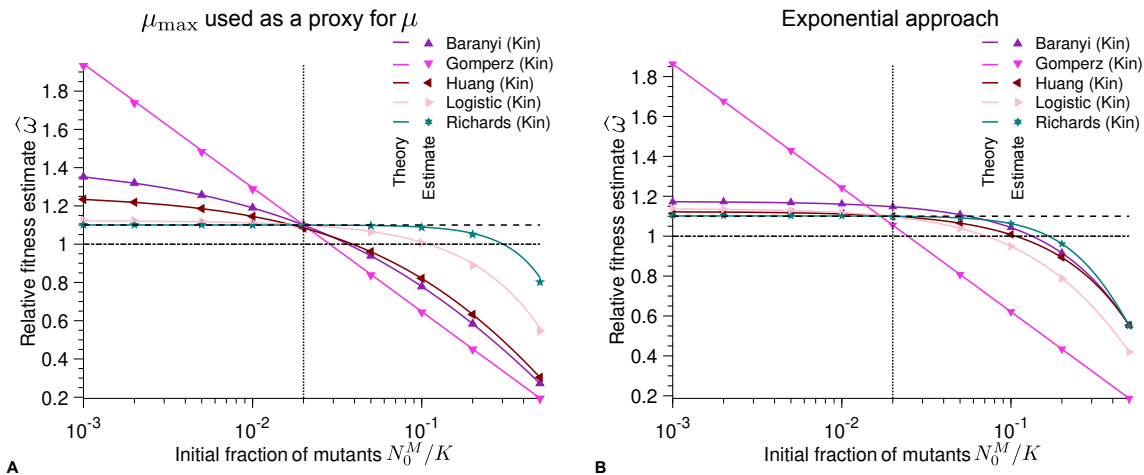


Figure 4: **Different initial population fractions between wild-type and mutant batch cultures result in poor estimates of relative fitness:** Relative fitness $\hat{\omega}$ estimate versus initial fraction $N_{0,M}/K$ of mutants for different kinetic population growth models. As a reminder, $\omega = \mu_M/\mu_{WT}$. **A) the maximum growth rate μ_{\max} is used as a proxy for the intrinsic growth rate μ .** Each point represents estimated values by Spline (growthrates package) from simulated data averaged over 10^4 stochastic realizations. The solid lines correspond to the analytical predictions of the relative fitness using estimates of the maximum growth rate (see Table 2). **B) the intrinsic growth rate is obtained applying the exponential approximation.** Solid lines correspond to the analytical predictions of the relative fitness using estimates of the maximum growth rate (see Table 3). In both panels the dashed line shows the real relative fitness value w . The dotted line represents the configuration in which the growth model parameters of the mutant are equal to the parameters of the wild-type (except their intrinsic growth rates). The dash-dotted line corresponds to the neutral case, i.e. when both the mutant and the wild-type have the same growth rate. Parameter values: $K_{WT} = K_M = K = 10^5$, $\mu_{WT} = 1$, $\mu_M = 1.1$, $\alpha_{WT} = \alpha_M = 2$, $\beta_{WT} = \beta_M = 2$, $h_{0,WT} = h_{0,M} = 2$, $\tau_{WT} = \tau_M = 2$ and $t = 1$.

556 to all methods we tested. For kinetic models (which are defined in terms of μ), we estimated
 557 μ_{\max} by using derivatives to find the maximum slope of $\ln(N/N_0)$ (as shown in Figure 1C;
 558 see Table 2).

559 The maximum growth rate (μ_{\max}) values estimated from the same data vary widely de-
 560 pending on the method used (Figure 5A, and Figures S1A, S2A and S3A). It is not possible to
 561 assess the accuracy of the estimates for the model-free methods. However, we used goodness-
 562 of-fit tests to assess the model-based methods by calculating the residual sum of squares
 563 (RSS). The RSS measures the discrepancy between the data and the fitted model. Thus, the
 564 smaller the RSS, the better the model. Since the models we tested have different numbers of
 565 parameters, we also calculated Akaike's Information Criterion (AIC) for kinetic models using
 566 the method of López et al. (2004). The results of the AIC are consistent with those of the
 567 RSS (see Supplementary Material). Despite the discrepancy in the inferred maximum growth
 568 rate, many of the models fit the data well in most cases because the RSS values are low and
 569 similar (Figures 5B-C, and Figures S1B-C, S2B-C and S3B-C).

570 A visual inspection of the fits corroborates our findings that all models fit the data gener-

571 ally well (visualizations of all fits available at available at <https://github.com/LcMrc/GrowthRates>).
572 We emphasize that a visual inspection is important to ensure that the estimated values are
573 appropriate. Indeed, in a few cases, the fits proved to be unsatisfactory although the summary
574 statistics were good (see, e.g., Figure S6).

575 No model is consistently preferred for all samples of a data-set. This highlights the dif-
576 ficulty of choosing ‘the one’ right model, although this choice has a great impact on the
577 growth parameter estimates. The Gompertz equation, whether statistical or kinetic, fre-
578 quently yielded the worst statistics, although our literature review indicates the statistical
579 Gompertz equation as the most frequently used model. Moreover, the models used in the
580 original publications of the data were not always the models that we found to obtain the best
581 statistics.

582 As previously stated, model-free methods may be preferred for some research questions,
583 especially when neither the underlying mechanisms nor relative fitness estimates are of in-
584 terest. Model-free methods obtain the maximum growth rate by determining the maximum
585 of the function $d \ln(N(t)/N_0)/dt$ (see Figure 1C). A quick comparison with the derivative of
586 the experimental data ensures the validity of the estimate. We found that Easy Linear gave
587 slightly different results from the Spline method because the former requires the user to spec-
588 ify how many data points to include for the analysis of the log-linear part of the growth curve.
589 Note that model-free methods are likely to be more accurate than model-based methods for
590 estimating μ_{\max} because the latter involve more parameters and a data fit.

591 **Relative growth rate estimates from empirical data:**

592 Adkar et al. (2017) used μ_{\max} estimates from a statistical Gompertz model in order to estimate
593 relative fitnesses. Therefore, this study allowed us to evaluate our concerns about using μ_{\max}
594 for relative fitness estimates. First, we used all approaches (model-free methods, statistical
595 models, and kinetic models) to estimate μ_{\max} for the wild-type and mutant strains from this
596 data-set. Assuming (erroneously) that μ_{\max} was a proxy for μ , we then calculated the relative
597 fitness. Figure 5D shows that kinetic models (circles) estimate more beneficial fitness values
598 than methods that estimate μ_{\max} directly (diamonds for model-free methods and squares for
599 statistical models). Especially for strains that were estimated by Adkar et al. 2017 (crosses)
600 to have especially low fitness, we found a large variation in the fitness values estimated by
601 different methods.

602 Next, we used kinetic models to estimate the intrinsic growth rate μ for the wild-type and
603 mutant strains from this data-set and subsequently calculated the relative fitness. In Figure
604 5E we compared our estimated values with those published by Adkar et al. (2017). Again,
605 many models estimate larger fitness values than those reported in the original study. This is
606 especially pronounced for samples that were estimated by Adkar et al. 2017 (crosses) to have
607 especially low fitness.

608 The overall conclusion of this section is that estimating relative fitness using inaccurate
609 estimates of μ likely propagates to the level of relative fitnesses, and causes large discrep-
610 ancies between relative fitness values estimated using different methods. Importantly, these
611 discrepancies are most pronounced for samples that are of special interest in an experiment.

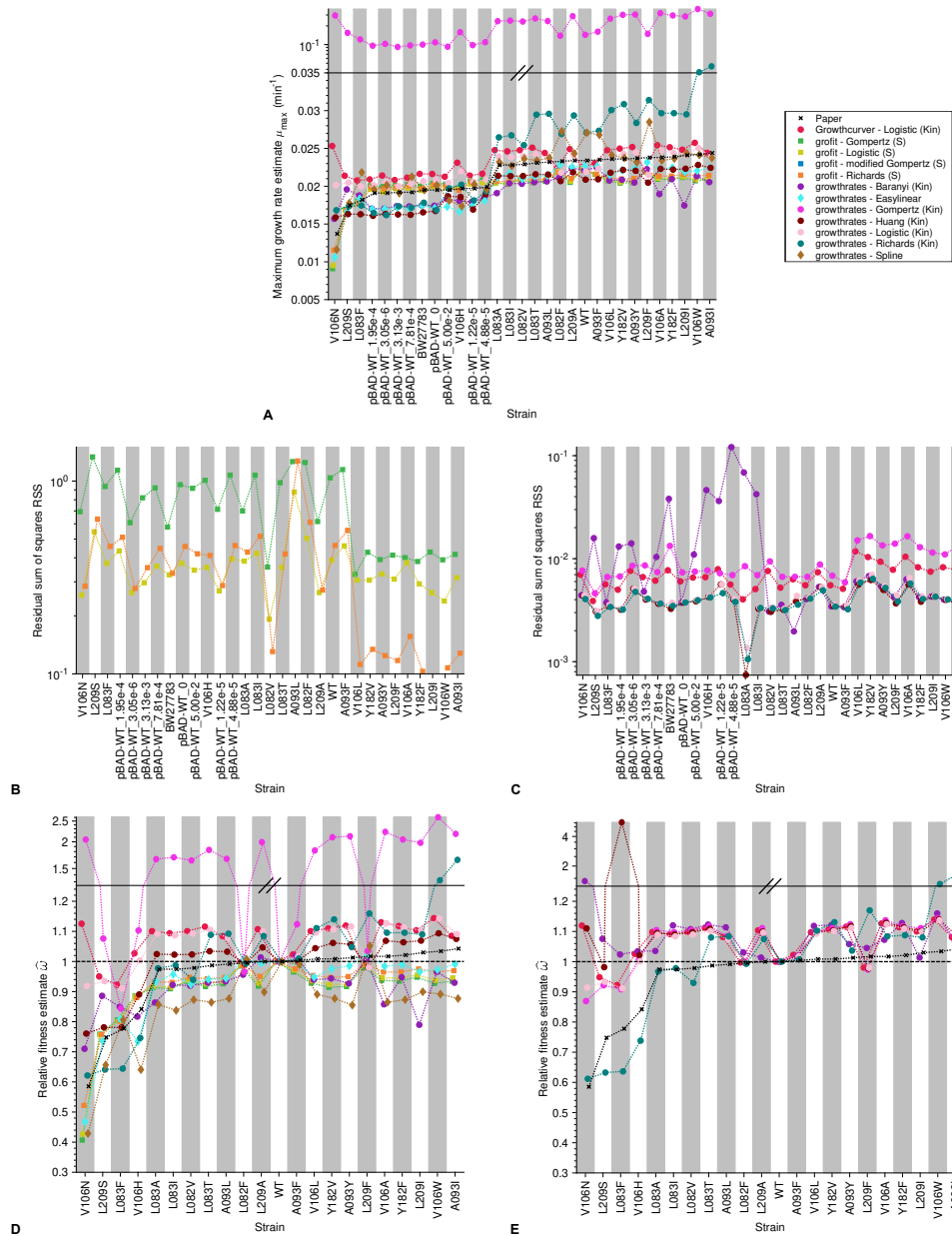


Figure 5: **Analysis of published data-sets (Adkar et al., 2017) shows that estimates differ vastly depending on the method:** A) Maximum growth rate $\hat{\mu}_{max}$ estimate for each strain. Each growth curve was analyzed using three different R packages including both model-free and model-based methods. The crosses show the values reported in the paper, the circles are obtained by methods based on kinetic models, the squares by methods based on statistical models and the diamonds by model-free methods. B) Goodness-of-fit measured as residual sum of squares (RSS) by strain for the statistical models. C) RSS by strain for the kinetic models. We include the RSS of statistical and kinetic models in different plots as the scale of the y-axes differ between these models: statistical models operate on a logarithmic scale since $y = \ln(N/N_0)$ but kinetic models operate on a linear scale $N(t)$. **Relative fitness:** D) and E) Relative fitness estimate $\hat{\omega}$ versus strain. In D) the relative fitness is computed using μ_{max} whereas in E) it is computed using μ .

612 **Implications of data re-analysis**

613 Our analysis indicates that the choice of the best method to analyze growth curve data is very
614 difficult. Especially, identifying the ‘right’ model that best fits all strains/treatments within
615 a data-set seems daunting. This difficulty might explain why there exists such a diversity of
616 methods for analyzing growth curve data, as we found in the literature review. Interestingly,
617 we saw that most articles only report using one method for analyzing their data. We suspect
618 that different labs and researchers have their own preferences and habits on how to obtain
619 growth rate estimates. In the interest of time (and sanity), researchers may be using the model
620 and method they know best and for which they have obtained reasonable-looking results in
621 the past, rather than trying out a multitude of unfamiliar computational tools.

622 One clear finding from our re-analysis of published data is that the Gompertz family of
623 models – both statistical and kinetic – are usually not the best choice. This point was previ-
624 ously made by López et al. (2004). We corroborate their empirical results with mathematical
625 arguments. However, our literature review showed that the Gompertz models have remained
626 popular long after López et al.’s study in 2004. We recommend that experimenters fit and
627 compare more than one model when analyzing data. In the light of our results, it will be im-
628 portant to develop one easy-to-use framework that allows for model choice and comparison,
629 which would easily single out inappropriate models.

630 Our results confirmed the finding of (Peleg and Corradini, 2011) that standard statistical
631 techniques for model selection were often unhelpful (Figure 5B-C): when comparing the fit of
632 different models to the same data, the goodness-of-fit statistics did not always select the model
633 that looked best upon visual inspection and/or there was not much difference between models
634 in terms of goodness-of-fit. This corroborates our personal communications with empiricists
635 that they are reluctant to use models for fitting their growth curve data.

636 **3 Recommendations & Conclusions**

637 Despite the long-established study of batch culture growth curve data, estimating growth
638 rates is still not straightforward. Using a literature review, math, simulations, and analysis of
639 previously published data, our work highlights experimental and theoretical pitfalls encoun-
640 tered by many researchers who work with batch monoculture growth curves. To that end,
641 we have summarized our recommendations for better growth rate estimates as a checklist in
642 Figure 6.

643 **General recommendations:**

644 We urge readers to remember that the intrinsic growth rate μ , a model parameter estimated
645 from kinetic models, is not the same as the maximum growth rate μ_{\max} , a statistical quantity
646 of data estimated using statistical models or by model-free methods. Although μ_{\max} is often
647 used as a proxy for μ , this assumption is not always justified.

648 We recommend that researchers make their raw data and methods available and repro-
649 ducible. In particular, this involves reporting all experimental parameters like inoculum size,
650 carrying capacity or initial fraction, and lag time. During our literature review, we were sur-
651 prised by the lack of sufficient information on experimental methods, estimated values, and
652 data availability.

653 **Experimental recommendations:**

654 Good data begin with good experimental methods. In the absence of a lag phase, the fastest

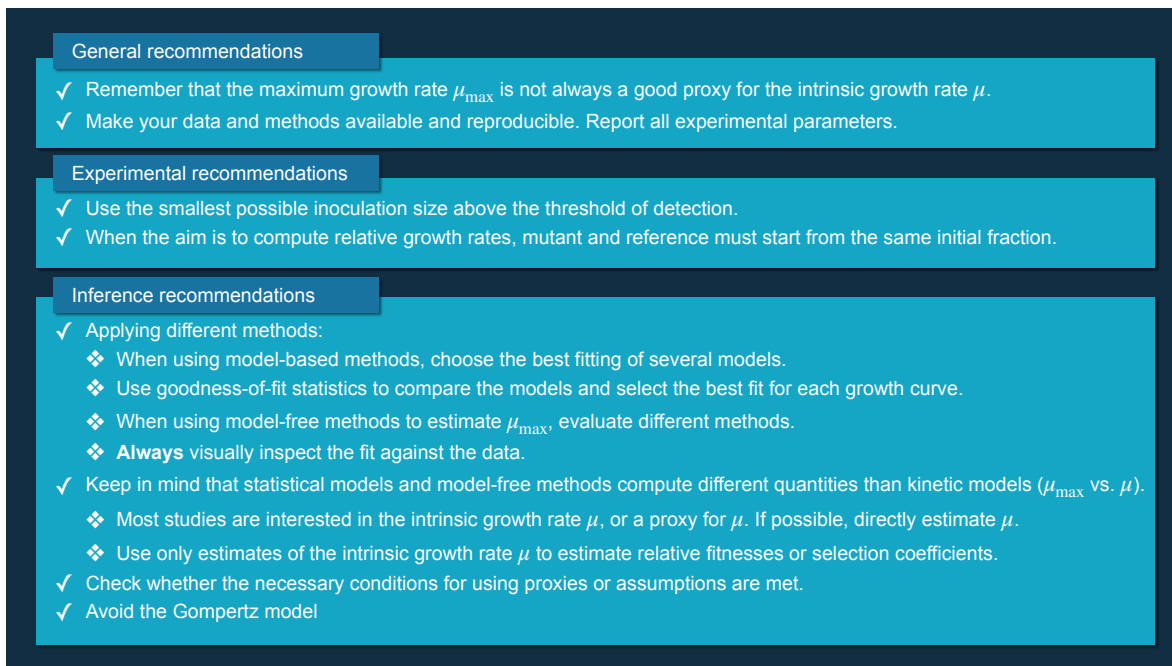


Figure 6: A list of recommendations for better growth rate inference from monoculture growth curves.

655 growth rate (both for the maximum growth rate μ_{\max} and for the intrinsic growth rate μ) is
656 observed at the very start of the growth curve. As we show in Figures 3A and 4, the estimates
657 of interest can be highly sensitive to the inoculum size. Also, when a lag phase is suspected,
658 reliable data from the start of the growth curve are necessary to quantify the lag time and
659 growth rate. Therefore, we recommend that experimenters use the smallest inoculation size
660 possible that is still reliably above the threshold of detection (if using a microplate reader,
661 follow the recommendations of Hall et al. 2014).

662 For accurate estimation of the relative growth rate, we stress that the mutant and reference/wild-
663 type strains should start from the same initial fraction ($N_0^M/K_M = N_0^{WT}/K_{WT}$; Figure 4),
664 which is not necessarily the same absolute size. If the strains have the same carrying capacity
665 ($K_M = K_{WT}$) at stationary phase, then it is possible to either dilute the cultures used for inoc-
666 ulation by the same dilution factor or begin the growth curves at the same absolute inoculum
667 size ($N_0^M = N_0^{WT}$). However, if the carrying capacities differ between strains, then the same
668 absolute inoculum size cannot be used. We found in our literature review that about half of
669 papers use a fixed absolute inoculum size to start their growth curve experiments whereas the
670 other half use a fixed dilution factor, usually without justifying either choice. We recommend
671 that experimenters interested in calculating relative growth rates use a fixed dilution factor.
672 A pilot experiment is ideal to inform on the carrying capacities and corresponding optimal
673 inoculum sizes.

674 **Inference recommendations:**

675 Regarding inference methods, our main recommendation is to try out several different methods
676 on the same data. We recommend that a computational method is used to estimate the growth
677 rate. (Manual) Fitting of an exponential model should be avoided (Table 3), regardless

678 of whether the exponential model is fit explicitly or implicitly by using the equation $R =$
679 $(\log_2 N_2 - \log_2 N_1)/(t_2 - t_1)$.

680 Model-free computational methods tend to be technically easier to use than model-based
681 methods, but they can only estimate μ_{\max} . If a model-free method is used, we recommend
682 to try different programs, ideally based on different algorithms. Model-based methods often
683 require more computational knowledge for fitting, but we still recommend that researchers
684 try to fit more than one model. We recommend this because, by re-analyzing previously
685 published data, we showed that there is not one model that fits best for all data-sets or even
686 one model that best fits every curve within a specific data-set (Figures 5B-C, S1B-C, S2B-C
687 and S3B-C). Therefore, it is important to select the best fitting model for each curve. For
688 those familiar with the R statistical programming language, we recommend the growthrates
689 package, because all of the kinetic models presented in Table 1, as well as model-free methods
690 for estimating μ_{\max} , can easily be fitted with this package. We recommend that researchers
691 use goodness-of-fit summary statistics (like the RSS, AIC, etc.) to compare models and select
692 the best fit. However, additional visual inspection of the estimated value and the data is
693 essential because goodness-of-fit statistics can be misleading (e.g., Figure S6).

694 Our work explains and demonstrates that and why the maximum growth rate μ_{\max} is
695 different from the intrinsic growth rate μ , which is a key point to take away and remember from
696 this paper. We suggest that researchers attempt to estimate μ directly from their data using
697 kinetic models. However, we have shown that it can be justified to use the statistical quantity
698 μ_{\max} as a proxy for the model parameter μ if certain conditions are met. We recommend
699 that experimenters decide which one makes more sense to use for the experimental question
700 at hand and, based on that decision, select the types of models or model-free approaches
701 to use. If μ_{\max} is to be inferred, model-free methods or fits of statistical models can be
702 used. Model-based methods can either be used to estimate the maximum growth rate μ_{\max}
703 of statistical models, or the intrinsic growth rate μ of kinetic models. We urge experimenters
704 not to compare estimates obtained from kinetic and statistical models because these different
705 model types estimate different growth rate parameters. Researchers should be aware that
706 confusion between the two quantities is common and different authors/fields use different
707 naming conventions. We hope that this paper provides readers with the necessary conceptual
708 understanding to critically navigate the literature. Finally, we note that only the intrinsic
709 growth rate μ (and not μ_{\max} or the exponential approximation) should be used for estimating
710 the relative fitness (Figure 4) from monoculture growth curves.

711 It is important to verify that the necessary conditions are met for the inference method(s)
712 to be used. For example, the exponential approximation should only be used when the
713 following assumptions are met: the inoculum size is much smaller than the carrying capacity
714 ($N_0 \ll K$, e.g., by at least 2 orders of magnitude), only time points at which the population
715 size remains much smaller than the carrying capacity are considered ($N(t) \ll K$), and the lag
716 time is very short or absent (e.g., $h_0 \ll 1$ for growth following a Baranyi model). Given these
717 restrictive assumptions, rather than demonstrating that the conditions for the exponential
718 approximation are met, it may be more feasible for researchers to directly fit one of the
719 kinetic models listed in Table 1. Another approximation that requires justification is the use
720 of μ_{\max} as a proxy for μ . This approximation is only valid for small initial population fractions
721 (Figure 3) and short (or absent) lag times. To demonstrate that this is the case, it is essential
722 that experimenters report the initial population fraction(s) and the lag time(s) when using
723 μ_{\max} as a proxy for μ .

724 Finally, we recommend that researchers avoid fitting the Gompertz model for both absolute
725 and relative estimates of μ . In our study, the kinetic Gompertz model consistently showed
726 wrong estimates for simulated data (Figures 3-4) and unusually large estimates for empirical
727 data (Figure 5).

728 4 Methods

729 4.1 Literature review

730 We quantified the most frequently used methods of analyzing growth curve data for extracting
731 summary statistics. To this end, we used Web of Knowledge and Google Scholar to search
732 for peer-reviewed papers in the evolution and ecology literature that gathered any type of
733 growth curve data proportional to the number of individuals growing in a homogeneous,
734 liquid culture and estimated growth parameters from those data. Papers that quantified
735 binary presence/absence of growth (e.g. to assay lag time or spore viability) were excluded.
736 Most papers were found because they cited one of the following growth curve methods papers,
737 Zwietering et al. (1990); Hall et al. (2014); Sprouffske and Wagner (2016); or Delaney et al.
738 (2013). From each paper, we extracted information about whether the method used to analyze
739 growth curves is explicitly cited or described, what type(s) of growth curve summary statistic
740 was used, whether a model-free or model-based approach was used, whether the growth rate is
741 from a statistical or kinetic approach, which model(s) were fitted (if no equation is given, then
742 the name of the model as reported by the author), whether the growth curves were inoculated
743 from a fixed starting value or as a fraction of the carrying capacity, and whether the growth
744 curve raw data are publicly available or, at least, plotted (summarized in table S1). For all
745 papers in which growth curves were inoculated using a fraction from overnight cultures, the
746 dilution factor was used as an estimator of the initial dilution fraction. If given, we extracted
747 the initial dilution factor and any accompanying information about the inoculum (e.g., length
748 of overnight culture) to indicate whether the dilution factor is a good proxy for the initial
749 population fraction (N_0/K). For papers in which growth curves were inoculated using a fixed
750 absolute number of cells, we report the dilution fraction only if sufficient information about
751 the inoculum size and carrying capacity was provided in the methods. Finally, we categorized
752 different model-free growth rate estimation methods that were applied *ad hoc* as either “Easy
753 Linear” if a consistent method was given for selecting which points to include in the regression
754 (since this is the main feature of popular model-free methods like that of Hall et al. 2014), or
755 as “exponential approximation” if there was no information about which points were included
756 in the regression or as “spline” if pairs of successive measurements were used to estimate the
757 local slope of the curve.

758 4.2 Analyzing 4 published data-sets

759 Data-sets appropriate for our analysis were found during our literature review and the data
760 were accessed as indicated in each paper.

761 We used the following R (version 4.1.1) packages to re-analyze the data: Growthcurver
762 (version 0.3.1), grofit (version 1.1.1-1) and growthrates (version 0.8.2). Each of them was
763 downloaded from the CRAN repository except grofit that we obtained from Kahm et al.
764 (2010). Indeed the latter was found to be removed from the CRAN repository. The package

765 Growthcurver is based on the kinetic logistic model, whereas grofit includes four statistical
766 models (Logistic, Gompertz, modified Gompertz and Richards). The package growthrates
767 provide both model-free methods (Easy Linear and Spline) as well as methods based on
768 kinetic models (Logistic, Gompertz, Richards, Baranyi and Huang).

769 We analyzed 143 population growth curves (31 from Adkar et al. 2017; 6 from Ram et al.
770 2019; 66 from Todd and Selmecki 2020; and 40 from Hammer et al. 2021) using all methods
771 mentioned above. We focused on the maximum growth rate μ_{\max} , because it is the only
772 quantity common to all models and methods. Since the kinetic models are defined based on
773 the intrinsic growth rate μ , we used Table 1 to calculate the maximum growth rate μ_{\max} from
774 the respective model.

To test the accuracy of the fits obtained by the model-based methods, we calculated the residual sum of squares (RSS). We used the definition from López et al. (2004):

$$\text{RSS} = \sum_{i=1}^n (OD_i - \widehat{OD}_i)^2.$$

775 Here, n is the number of data points, OD_i is the i^{th} optical density value to be estimated
776 and \widehat{OD}_i is the i^{th} estimated optical density value. Since the models have different numbers
777 of parameters, we also calculated the Akaike's Information Criterion (AIC) for the kinetic
778 models as given in López et al. (2004) and explained in the supplementary methods.

779

780 4.3 Simulations

781 We generated data representing the dynamics of microbial populations using a Gillespie al-
782 gorithm for the kinetic Gompertz, Richards and Logistic models (Gillespie, 1976, 1977). For
783 the Baranyi and Huang models, a modified Next-Reaction algorithm was required since these
784 models have time-dependent growth rates (Anderson, 2007). All simulation code was writ-
785 ten in C and is available at <https://github.com/LcMrc/GrowthRates>. We detail below the
786 algorithms used.

787 **Gillespie algorithm:** Let us denote by N the number of individuals. The only elementary
788 event that can happen is division of a microbe, whose rate is denoted by $k_{N \rightarrow N+1}$. Let us note
789 that $k_{N \rightarrow N+1} = \mu \log(K/N)N$, $k_{N \rightarrow N+1} = \mu(1 - N/K)N$ and $k_{N \rightarrow N+1} = \mu(1 - (N/K)^\beta)N$
790 for the kinetic Gompertz, Logistic and Richards models, respectively. Simulation steps are as
791 follows:

- 792 1. Initialization: The population starts from N_0 microorganisms at time $t = 0$.
- 793 2. Time update: The time increment Δt is sampled randomly from an exponential distri-
794 bution with mean $1/k_{N \rightarrow N+1}$ and the time t is updated such that $t \leftarrow t + \Delta t$.
- 795 3. Number of individuals update: a division occurs and the population size N increases by
796 one such that $N \leftarrow N + 1$.
- 797 4. We go back to Step 2 and iterate until the desired time limit is reached.

798 **Next-Reaction algorithm:** Let us denote by N the number of individuals. The only
799 elementary event that can happen is division of a microbe, whose time-dependent rate is
800 denoted by $k_{N \rightarrow N+1}(t)$. Let us note that $k_{N \rightarrow N+1}(t) = \mu e^{\mu t} (1 - N/K) N / (e^{h_0} - 1 + e^{\mu t})$
801 and $k_{N \rightarrow N+1}(t) = \mu (1 - N/K) N / (1 + e^{\alpha(t-\tau)})$ for the kinetic Baranyi and Huang models,
802 respectively. In the following, we will denote by P the first firing time and T the internal
803 time.

804 1. Initialization: The population starts from N_0 microorganisms at time $t = 0$. The first
805 firing time P is sampled from an exponential distribution of mean 1 and the internal
806 time T is set to 0.

807 2. Time update: The time increment Δt is computed solving $\int_t^{t+\Delta t} k_{N \rightarrow N+1}(u) du = P - T$
808 and the time t is updated such that $t \leftarrow t + \Delta t$.

809 3. Number of individuals update: a division occurs and the population size N increases by
810 one such that $N \leftarrow N + 1$.

811 4. Internal time update: The internal time T is updated such that $T \leftarrow T + \Delta T$, where
812
$$\Delta T = \int_t^{t+\Delta t} k_{N \rightarrow N+1}(u) du.$$

813 5. First firing time update: The first firing time P is updated such that $P \leftarrow P + \Delta P$,
814 where ΔP is sampled from an exponential distribution of mean 1.

815 6. We go back to Step 2 and iterate until the desired time limit is reached.

816 4.4 Data availability

817 The authors state that all data necessary for confirming the conclusions presented in the article
818 are represented fully within the article or Supplemental Material. Annotated C implemen-
819 tations of numerical simulations, annotated code to reproduce all computationally produced
820 graphs, and additional figures and tables reporting the data re-analysis fits and estimates are
821 available at <https://github.com/LcMrc/GrowthRates>.

822 5 Author Contributions

823 All authors designed the study; AHG performed the literature review; LM performed the
824 numerical and analytical work; all authors analyzed and interpreted the data; all authors
825 wrote and edited the manuscript.

826 6 Acknowledgements

827 The authors thank the Evolutionary Biology group at IGC for stimulating discussions and
828 the THEE Group at UniBe for feedback on the manuscript. AHG thanks FCT PhD funding
829 grant PD/BD/138215/2018. CB is grateful for funding from ERC Starting Grant 804569
830 (FIT2GO) and SNSF Project Grant “MiCo4Sys”.

831 References

- 832 Tanita Wein and Tal Dagan. The effect of population bottleneck size and selective regime
833 on genetic diversity and evolvability in bacteria. *Genome biology and evolution*, 11(11):
834 3283–3290, 2019.
- 835 Lindi M Wahl and Anna Dai Zhu. Survival probability of beneficial mutations in bacterial
836 batch culture. *Genetics*, 200(1):309–320, 2015. doi: 10.1534/genetics.114.172890.
- 837 Thomas E Miller, Jean H Burns, Pablo Munguia, Eric L Walters, Jamie M Kneitel, Paul M
838 Richards, Nicolas Mouquet, and Hannah L Buckley. A critical review of twenty years’ use
839 of the resource-ratio theory. *The American Naturalist*, 165(4):439–448, 2005.
- 840 Joey R Bernhardt, Pavel Kratina, Aaron Louis Pereira, Manu Tamminen, Mridul K Thomas,
841 and Anita Narwani. The evolution of competitive ability for essential resources. *Philosophical
842 Transactions of the Royal Society B*, 375(1798):20190247, 2020.
- 843 J Monod. The growth of bacterial cultures. *Annual Review of Microbiology*, 3(1):371—394,
844 1949. doi: 10.1146/annurev.mi.03.100149.002103.
- 845 Jeniffer Concepción-Acevedo, Howard N Weiss, Waqas Nasir Chaudhry, and Bruce R Levin.
846 Malthusian parameters as estimators of the fitness of microbes: a cautionary tale about the
847 low side of high throughput. *PloS one*, 10(6):e0126915, 2015.
- 848 Yoav Ram, Eynat Dellus-Gur, Maayan Bibi, Kedar Karkare, Uri Obolski, Marcus W. Feld-
849 man, Tim F. Cooper, Judith Berman, and Lilach Hadany. Predicting microbial growth
850 in a mixed culture from growth curve data. *Proceedings of the National Academy of Sci-
851 ences*, 116(29):14698–14707, 2019. ISSN 0027-8424. doi: 10.1073/pnas.1902217116. URL
852 <https://www.pnas.org/content/116/29/14698>.
- 853 Michael Knopp and Dan I Andersson. Predictable phenotypes of antibiotic resistance muta-
854 tions. *MBio*, 9(3):e00770–18, 2018.
- 855 Arthur Slator. Ii. the rate of growth of bacteria. *J. Chem. Soc., Trans.*, 109:2–10, 1916. doi:
856 10.1039/CT9160900002. URL <http://dx.doi.org/10.1039/CT9160900002>.
- 857 Tor Carlson. Über geschwindigkeit und grösse der hefevermehrung in würze. *Biochem. Ztschr.
858 Bd.*, 57:313–334, 1913.
- 859 Nigel F Delaney, Maria E Kaczmarek, Lewis M Ward, Paige K Swanson, Ming-Chun Lee, and
860 Christopher J Marx. Development of an optimized medium, strain and high-throughput
861 culturing methods for *Methylobacterium extorquens*. *PLoS One*, 8(4):e62957, 2013.
- 862 Barry G Hall, Hande Acar, Anna Nandipati, and Miriam Barlow. Growth rates made easy.
863 *Molecular biology and evolution*, 31(1):232–238, 2014.
- 864 Keiran Stevenson, Alexander F McVey, Ivan BN Clark, Peter S Swain, and Teuta Pilizota.
865 General calibration of microbial growth in microplate readers. *Scientific reports*, 6(1):1–7,
866 2016.

- 867 Masaomi Kurokawa and Bei-Wen Ying. Precise, high-throughput analysis of bacterial growth.
868 *Journal of Visualized Experiments: JoVE*, 127:e56197, 2017.
- 869 M. H. Zwietering, I. Jongenburger, F. M. Rombouts, and K. Van't Riet. Modeling of the
870 bacterial growth curve. *Applied and environmental microbiology*, 56(6):1875–1881, 1990.
- 871 József Baranyi and Terry A. Roberts. A dynamic approach to predicting bacte-
872 rial growth in food. *International Journal of Food Microbiology*, 23(3):277–294,
873 1994. ISSN 0168-1605. doi: [https://doi.org/10.1016/0168-1605\(94\)90157-0](https://doi.org/10.1016/0168-1605(94)90157-0). URL
874 <https://www.sciencedirect.com/science/article/pii/0168160594901570>. Special
875 Issue Predictive Modelling.
- 876 Paul P Jung, Nils Christian, Daniel P Kay, Alexander Skupin, and Carole L Linster. Protocols
877 and programs for high-throughput growth and aging phenotyping in yeast. *PloS one*, 10
878 (3):e0119807, 2015.
- 879 Anders Blomberg. Measuring growth rate in high-throughput growth phenotyping. *Current*
880 *Opinion in Biotechnology*, 22(1):94–102, 2011.
- 881 Kathleen Sprouffske and Andreas Wagner. Growthcurver: an R package for ob-
882 taining interpretable metrics from microbial growth curves. *BMC Bioinformat-*
883 *ics*, 17(1):172, 4 2016. ISSN 1471-2105. doi: 10.1186/s12859-016-1016-7. URL
884 <https://doi.org/10.1186/s12859-016-1016-7>.
- 885 Thomas Petzoldt. *growthrates: Estimate Growth Rates from Experimental Data*, 2020. URL
886 <https://CRAN.R-project.org/package=growthrates>. R package version 0.8.2; A collec-
887 tion of methods to determine growth rates from experimental data, in particular from batch
888 experiments and plate reader trials.
- 889 Mark D Wilkinson, Michel Dumontier, IJsbrand Jan Aalbersberg, Gabrielle Appleton, Myles
890 Axton, Arie Baak, Niklas Blomberg, Jan-Willem Boiten, Luiz Bonino da Silva Santos,
891 Philip E Bourne, et al. The FAIR guiding principles for scientific data management and
892 stewardship. *Scientific data*, 3(1):1–9, 2016.
- 893 Marcus R Munafò, Brian A Nosek, Dorothy VM Bishop, Katherine S Button, Christopher D
894 Chambers, Nathalie Percie du Sert, Uri Simonsohn, Eric-Jan Wagenmakers, Jennifer J
895 Ware, and John Ioannidis. A manifesto for reproducible science. *Nature human behaviour*,
896 1(1):1–9, 2017.
- 897 Erik Gullberg, Sha Cao, Otto G Berg, Carolina Ilbäck, Linus Sandegren, Diarmaid Hughes,
898 and Dan I Andersson. Selection of resistant bacteria at very low antibiotic concentrations.
899 *PLOS Pathogens*, 7(7):e1002158, 2011.
- 900 Sandra Trindade, Ana Sousa, and Isabel Gordo. Antibiotic resistance and stress in the light
901 of fisher’s model. *Evolution*, 66(12):3815–3824, 2012.
- 902 Luciano Fernandez-Ricaud, Olga Kourtchenko, Martin Zackrisson, Jonas Warringer, and An-
903 ders Blomberg. Precog: a tool for automated extraction and visualization of fitness com-
904 ponents in microbial growth phenomics. *BMC Bioinformatics*, 17(1):1–15, 2016.

- 905 Portia Mira, Miriam Barlow, Juan C Meza, and Barry G Hall. Statistical package for
906 growth rates made easy. *Molecular biology and evolution*, 34(12):3303–3309, 2017. doi:
907 <https://doi.org/10.1093/molbev/msx255>.
- 908 Kazuha Ashino, Kenta Sugano, Toshiyuki Amagasa, and Bei-Wen Ying. Predicting the de-
909 cision making chemicals used for bacterial growth. *Scientific reports*, 9:7251, 2019. doi:
910 <https://doi.org/10.1038/s41598-019-43587-8>.
- 911 Matthias Kahm, Guido Hasenbrink, Hella Lichtenberg-Fraté, Jost Ludwig, and
912 Maik Kschischo. grofit: Fitting biological growth curves with R. *Jour-
913 nal of Statistical Software*, 33(7):1–21, 2010. doi: 10.18637/jss.v033.i07. URL
914 <https://www.jstatsoft.org/index.php/jss/article/view/v033i07>.
- 915 Sarah P Otto and Troy Day. *A biologist’s guide to mathematical modeling in ecology and
916 evolution*. Princeton University Press, 2011.
- 917 Benjamin M Bolker. *Ecological models and data in R*. Princeton University Press, 2008.
- 918 Benoît Chezeau and Christophe Vial. *Modeling and Simulation of the Biohydrogen Production
919 Processes*, chapter 19, pages 445–483. Elsevier B.V. All, 2019. doi: 10.1016/C2017-0-03531-
920 0.
- 921 A. Tsoularis and J. Wallace. Analysis of logistic growth models. *Mathematical Biosciences*,
922 179(1):21–55, 2002. ISSN 0025-5564. doi: [https://doi.org/10.1016/S0025-5564\(02\)00096-2](https://doi.org/10.1016/S0025-5564(02)00096-2).
923 URL <https://www.sciencedirect.com/science/article/pii/S0025556402000962>.
- 924 Lihan Huang. A new mechanistic growth model for simultaneous determination of lag
925 phase duration and exponential growth rate and a new bēlehrádek-type model for
926 evaluating the effect of temperature on growth rate. *Food Microbiology*, 28(4):770–
927 776, 2011. ISSN 0740-0020. doi: <https://doi.org/10.1016/j.fm.2010.05.019>. URL
928 <https://www.sciencedirect.com/science/article/pii/S0740002010001255>. Predic-
929 tive Modeling in Foods.
- 930 Stefano Perni, Peter W. Andrew, and Gilbert Shama. Estimating the maximum growth
931 rate from microbial growth curves: definition is everything. *Food Microbiology*, 22(6):
932 491–495, 2005. ISSN 0740-0020. doi: <https://doi.org/10.1016/j.fm.2004.11.014>. URL
933 <https://www.sciencedirect.com/science/article/pii/S0740002004001522>.
- 934 Ru-Jun Yang, Xiu-Lin Wang, Ying-Ying Zhang, and Yu-Jie Zhan. Influence of cell equivalent
935 spherical diameter on the growth rate and cell density of marine phytoplankton. *Journal
936 of experimental marine biology and ecology*, 331(1):33–40, 2006.
- 937 Xueqing Wu, Nathan T Jacobs, Catherine Bozio, Preston Palm, Santiago M Lattar, Chris-
938 tiane R Hanke, David M Watson, Fuminori Sakai, Bruce R Levin, Keith P Klugman,
939 et al. Competitive dominance within biofilm consortia regulates the relative distribution
940 of pneumococcal nasopharyngeal density. *Applied and environmental microbiology*, 83(16):
941 e00953–17, 2017.
- 942 Sadia Khan, Tara K Beattie, and Charles W Knapp. The use of minimum selectable concentra-
943 tions (MSCs) for determining the selection of antimicrobial resistant bacteria. *Ecotoxicology*,
944 26(2):283–292, 2017.

- 945 Bharat V. Adkar, Michael Manhart, Sanchari Bhattacharyya, Jian Tian, Michael Mushar-
946 bash, and Eugene I. Shakhnovich. Optimization of lag phase shapes the evolution of a
947 bacterial enzyme. *Nature Ecology & Evolution*, 1(6):0149, 4 2017. ISSN 2397-334X. doi:
948 10.1038/s41559-017-0149. URL <https://doi.org/10.1038/s41559-017-0149>.
- 949 Donatella Ganucci, Simona Guerrini, Silvia Mangani, Massimo Vincenzini, and Lisa Granchi.
950 Quantifying the effects of ethanol and temperature on the fitness advantage of predominant
951 *Saccharomyces cerevisiae* strains occurring in spontaneous wine fermentations. *Frontiers*
952 *in microbiology*, 9:1563, 2018.
- 953 Nigel Delaney. Curve Fitter - software for growth curve fitting and visualization, 2014.
954 <http://www.evolvedmicrobe.com/CurveFitter/> [Accessed: 2021-11-23].
- 955 R. Kassen. *Experimental Evolution and the Nature of Biodiversity*. Macmillan Learning, 2014.
956 ISBN 9781936221462. URL <https://books.google.ch/books?id=LL8YnwEACAAJ>.
- 957 Prabh Basra, Ahlam Alsaadi, Gabriela Bernal-Astrain, Michael Liam O’Sullivan, Bryn Ha-
958 zlett, Leah Marie Clarke, Andrew Schoenrock, Sylvain Pitre, and Alex Wong. Fitness
959 tradeoffs of antibiotic resistance in extraintestinal pathogenic *Escherichia coli*. *Genome*
960 *biology and evolution*, 10(2):667–679, 2018.
- 961 Maja Novak, Thomas Pfeiffer, Martin Ackermann, and Sebastian Bonhoeffer. Bacterial
962 growth properties at low optical densities. *Antonie Van Leeuwenhoek*, 96(3):267–274, 2009.
- 963 Richard E. Lenski, Michael R. Rose, Suzanne C. Simpson, and Scott C. Tadler. Long-
964 term experimental evolution in escherichia coli. i. adaptation and divergence dur-
965 ing 2,000 generations. *The American Naturalist*, 138(6):1315–1341, 1991. URL
966 <http://www.jstor.org/stable/2462549>. Full publication date: Dec., 1991.
- 967 J.F. Crow and M. Kimura. *An Introduction to Population Genetics Theory*. Blackburn Press,
968 2009. ISBN 9781932846126. URL <https://books.google.pn/books?id=VWqKPwAACAAJ>.
- 969 Luis-Miguel Chevin. On measuring selection in experimental evolution. *Bi-*
970 *ology Letters*, 7(2):210–213, 2011. doi: 10.1098/rsbl.2010.0580. URL
971 <https://royalsocietypublishing.org/doi/abs/10.1098/rsbl.2010.0580>.
- 972 Tobin J. Hammer, Eli Le, and Nancy A. Moran. Thermal niches of specialized
973 gut symbionts: the case of social bees. *Proceedings of the Royal Society B: Bi-*
974 *ological Sciences*, 288(1944):20201480, 2021. doi: 10.1098/rspb.2020.1480. URL
975 <https://royalsocietypublishing.org/doi/abs/10.1098/rspb.2020.1480>.
- 976 Robert T Todd and Anna Selmecki. Expandable and reversible copy number amplification
977 drives rapid adaptation to antifungal drugs. *eLife*, 9:e58349, 7 2020. ISSN 2050-084X. doi:
978 10.7554/eLife.58349. URL <https://doi.org/10.7554/eLife.58349>.
- 979 S. López, M. Prieto, J. Dijkstra, M.S. Dhanoa, and J. France. Statistical evaluation of
980 mathematical models for microbial growth. *International Journal of Food Microbiology*, 96
981 (3):289–300, 2004. ISSN 0168-1605. doi: <https://doi.org/10.1016/j.ijfoodmicro.2004.03.026>.
982 URL <https://www.sciencedirect.com/science/article/pii/S0168160504002041>.

983 Micha Peleg and Maria G Corradini. Microbial growth curves: what the models tell us and
984 what they cannot. *Critical reviews in food science and nutrition*, 51(10):917–945, 2011.

985 Daniel T Gillespie. A general method for numerically simulating the stochastic time
986 evolution of coupled chemical reactions. *Journal of Computational Physics*, 22(4):403–
987 434, 1976. ISSN 0021-9991. doi: [https://doi.org/10.1016/0021-9991\(76\)90041-3](https://doi.org/10.1016/0021-9991(76)90041-3). URL
988 <https://www.sciencedirect.com/science/article/pii/0021999176900413>.

989 Daniel T. Gillespie. Exact stochastic simulation of coupled chemical reactions. *The Jour-*
990 *nal of Physical Chemistry*, 81(25):2340–2361, 1977. doi: 10.1021/j100540a008. URL
991 <https://doi.org/10.1021/j100540a008>.

992 David F. Anderson. A modified next reaction method for simulating chemical systems with
993 time dependent propensities and delays. *The Journal of Chemical Physics*, 127(21):214107,
994 2007. doi: 10.1063/1.2799998. URL <https://doi.org/10.1063/1.2799998>.

Supplement for: Challenges and pitfalls of inferring microbial growth rates from lab cultures

Ana-Hermina Ghenu^{*1,2,3}, Loïc Marrec^{†2,3}, and Claudia Bank^{1,2,3}

¹Instituto Gulbenkian de Ciência, Rua da Quinta Grande 6, Oeiras, 2780-156, Portugal

²Institut für Ökologie und Evolution, Universität Bern, Baltzerstrasse 6, CH-3012 Bern, Switzerland

³Swiss Institute of Bioinformatics, 1015 Lausanne, Switzerland

June 24, 2022

1 Supplementary methods

As explained in the main text, we re-analyzed the population growth curves from previously published data sets by fitting many different models and calculating the residual sum of squares (RSS). Since the models have different numbers of parameters, we also calculated the Akaike's Information Criterion (AIC) for the kinetic models giving $N(t)$, which reads

$$\text{AIC} = n \ln \left(\frac{\text{RSS}}{n} \right) + 2(p+1) + \frac{2(p+1)(p+2)}{n-p-2}, \quad (1)$$

where p is the number of parameters (López et al. 2004).

However, this equation may not be valid for the statistical models because these models are on a logarithmic scale ($y = \ln(N/N_0)$) and therefore the errors around the data are probably not normally distributed as assumed by López et al. 2004.

*Co-first and co-corresponding author: hermina.ghenu@gmail.com

†Co-first and co-corresponding author: loic.marrec@iee.unibe.ch

2 Supplementary figures

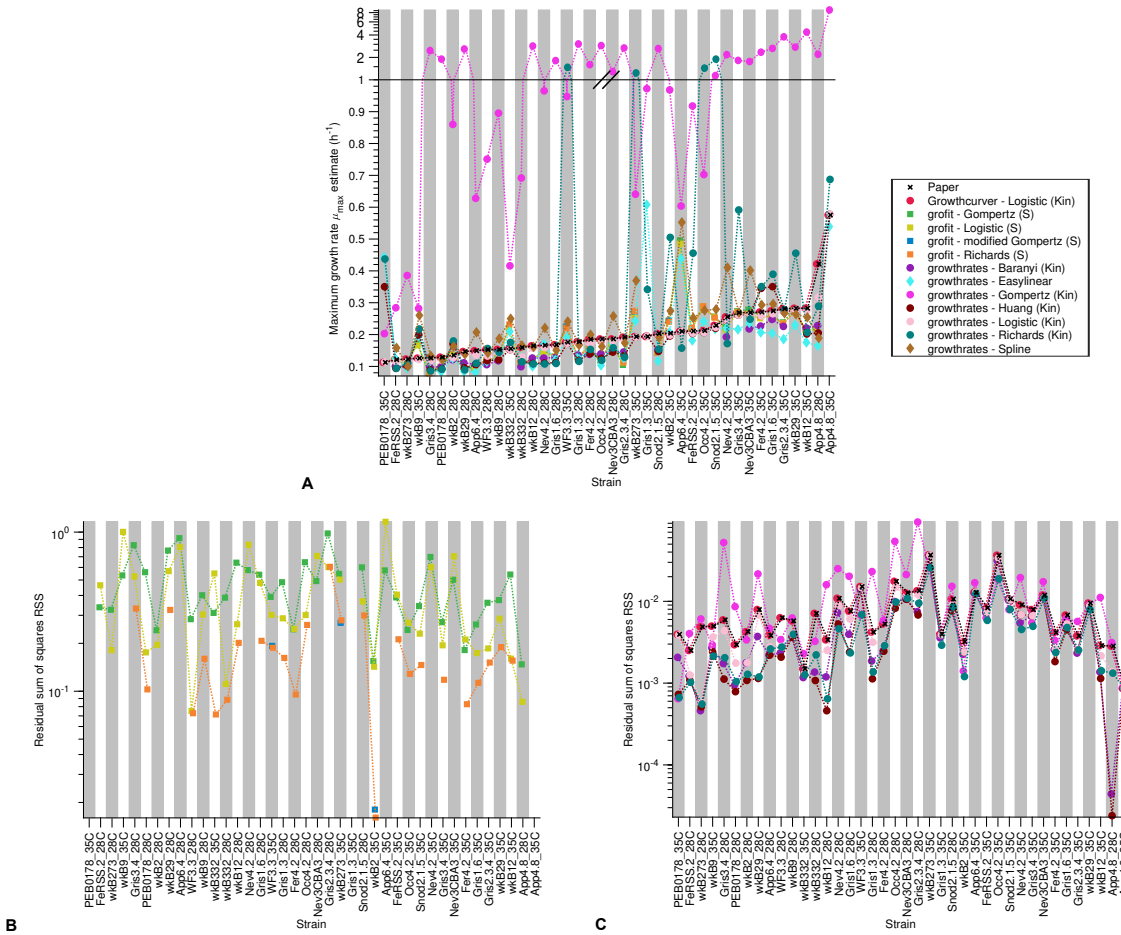


Figure S1: **Analysis of published data sets - Hammer, Le, and Moran 2021:** A) Maximum growth rate $\hat{\mu}_{\max}$ estimate versus strain. Each growth curve was analyzed using three different R packages including both model-free and model-based methods. The crosses show the values reported in the paper, the circles are obtained by methods based on kinetic models, the squares by methods based on statistical models and the diamonds by model-free methods. B) Residual sum of squares RSS versus strain for the statistical models. C) Residual sum of squares RSS versus strain for the kinetic models.

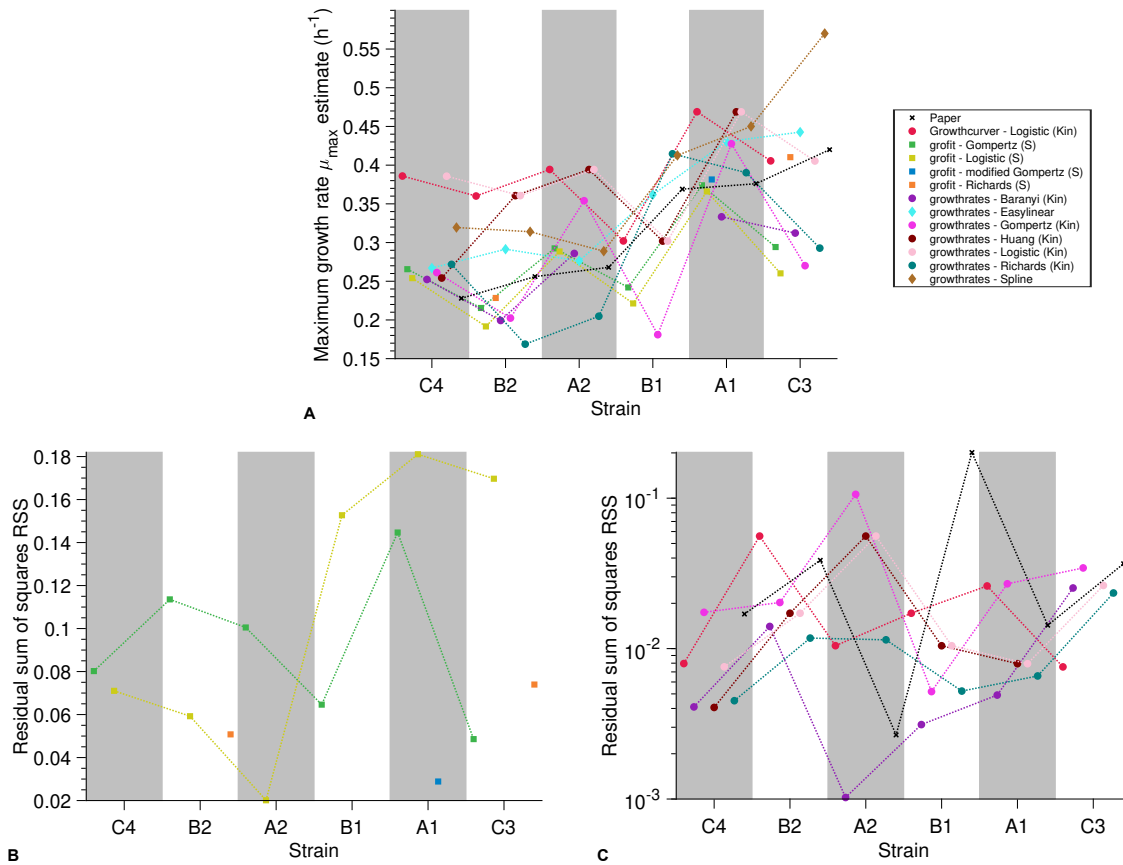


Figure S2: **Analysis of published data sets - Ram2019:** A) Maximum growth rate $\hat{\mu}_{\max}$ estimate versus strain. Each growth curve was analyzed using three different R packages including both model-free and model-based methods. The crosses show the values reported in the paper, the circles are obtained by methods based on kinetic models, the squares by methods based on statistical models and the diamonds by model-free methods. B) Residual sum of squares RSS versus strain for the statistical models. C) Residual sum of squares RSS versus strain for the kinetic models.

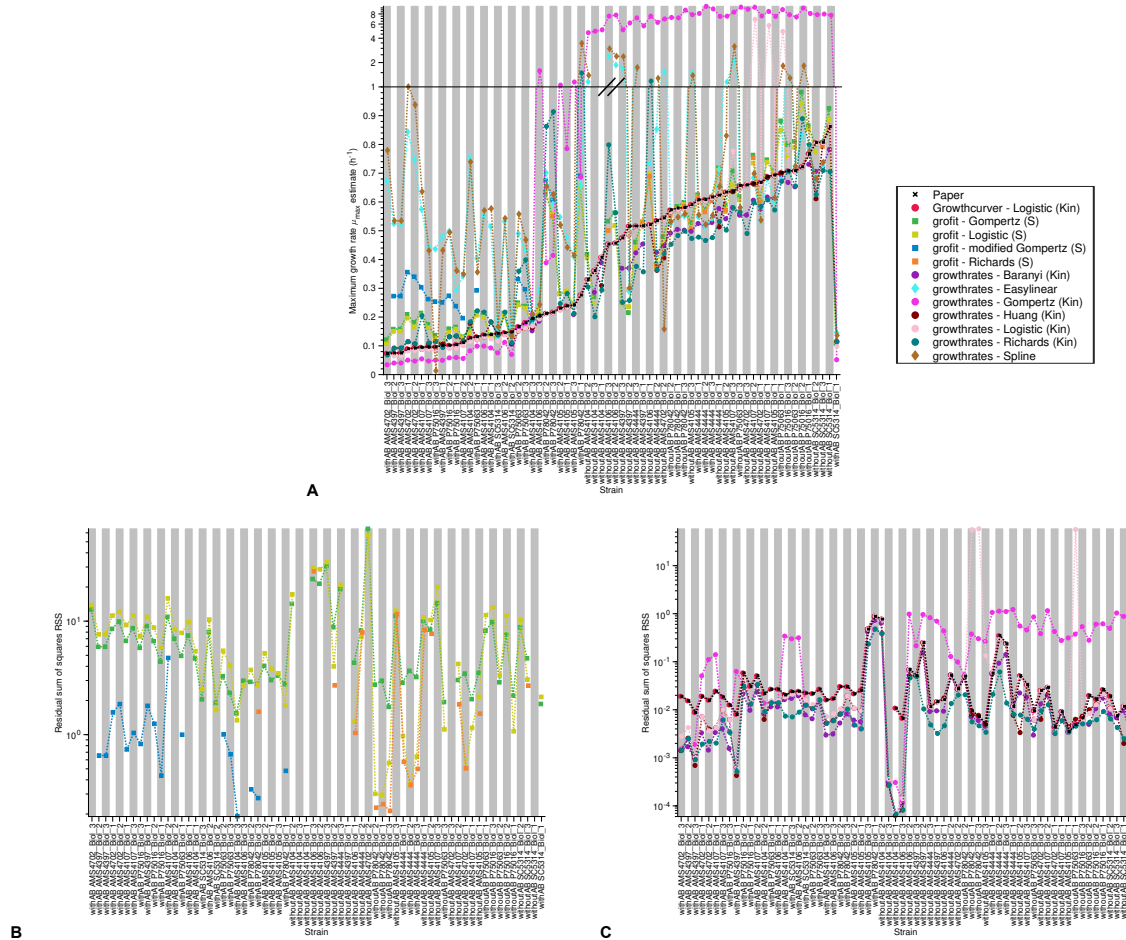


Figure S3: **Analysis of published data sets - Todd and Selmecki 2020:** A) Maximum growth rate $\hat{\mu}_{\max}$ estimate versus strain. Each growth curve was analyzed using three different R packages including both model-free and model-based methods. The crosses show the values reported in the paper, the circles are obtained by methods based on kinetic models, the squares by methods based on statistical models and the diamonds by model-free methods. B) Residual sum of squares RSS versus strain for the statistical models. C) Residual sum of squares RSS versus strain for the kinetic models.

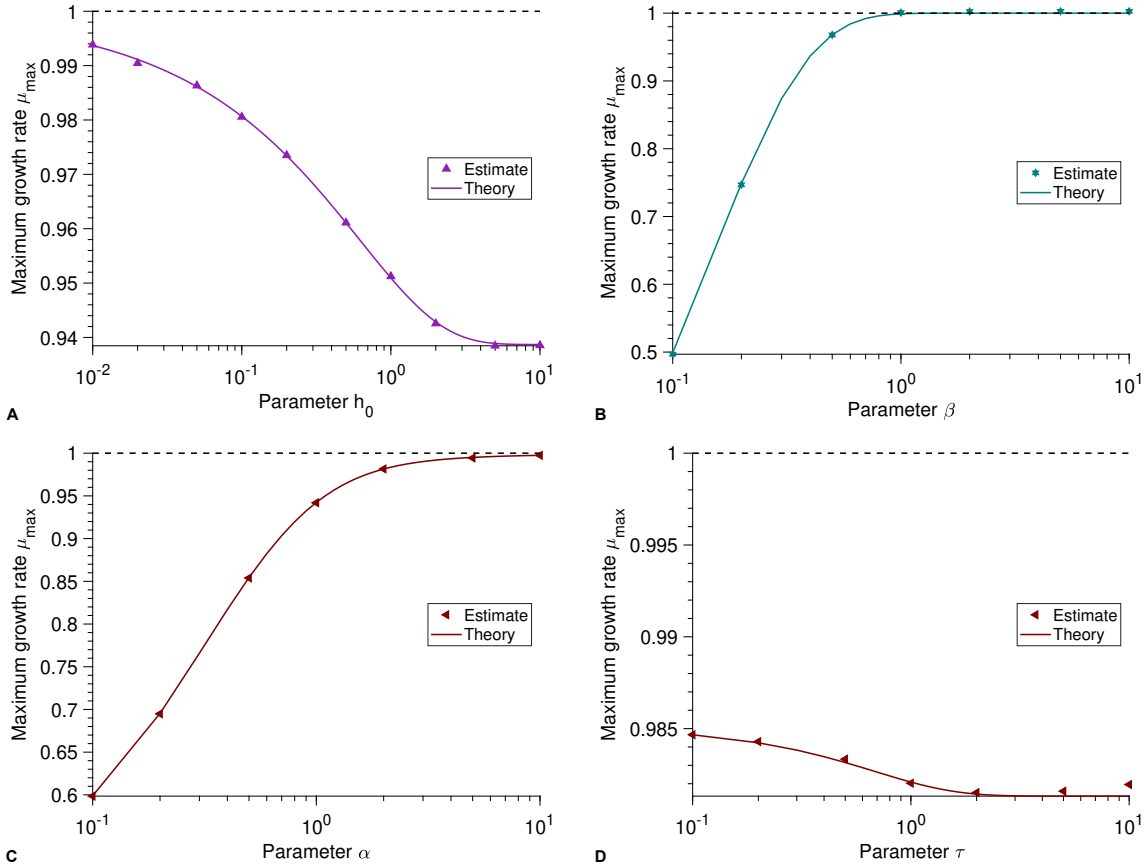


Figure S4: **Maximum growth rate:** A) Maximum growth rate μ_{\max} versus parameter h_0 for the Baranyi model. B) Maximum growth rate μ_{\max} versus parameter β for the Richards model. C) Maximum growth rate μ_{\max} versus parameter α for the Huang model. D) Maximum growth rate μ_{\max} versus parameter τ for the Huang model. In every panel, each point represents estimated values from simulated data averaged over 10^4 stochastic realizations. The solid lines correspond to the analytical predictions of the maximum growth rate (see Table 2 in the main text). The dashed line shows the intrinsic growth rate value μ . Parameter values: $N_0 = 10^2$, $K = 10^5$, $\mu = 1$, $\alpha = 2$ for panel D and $\tau = 2$ for panel C.

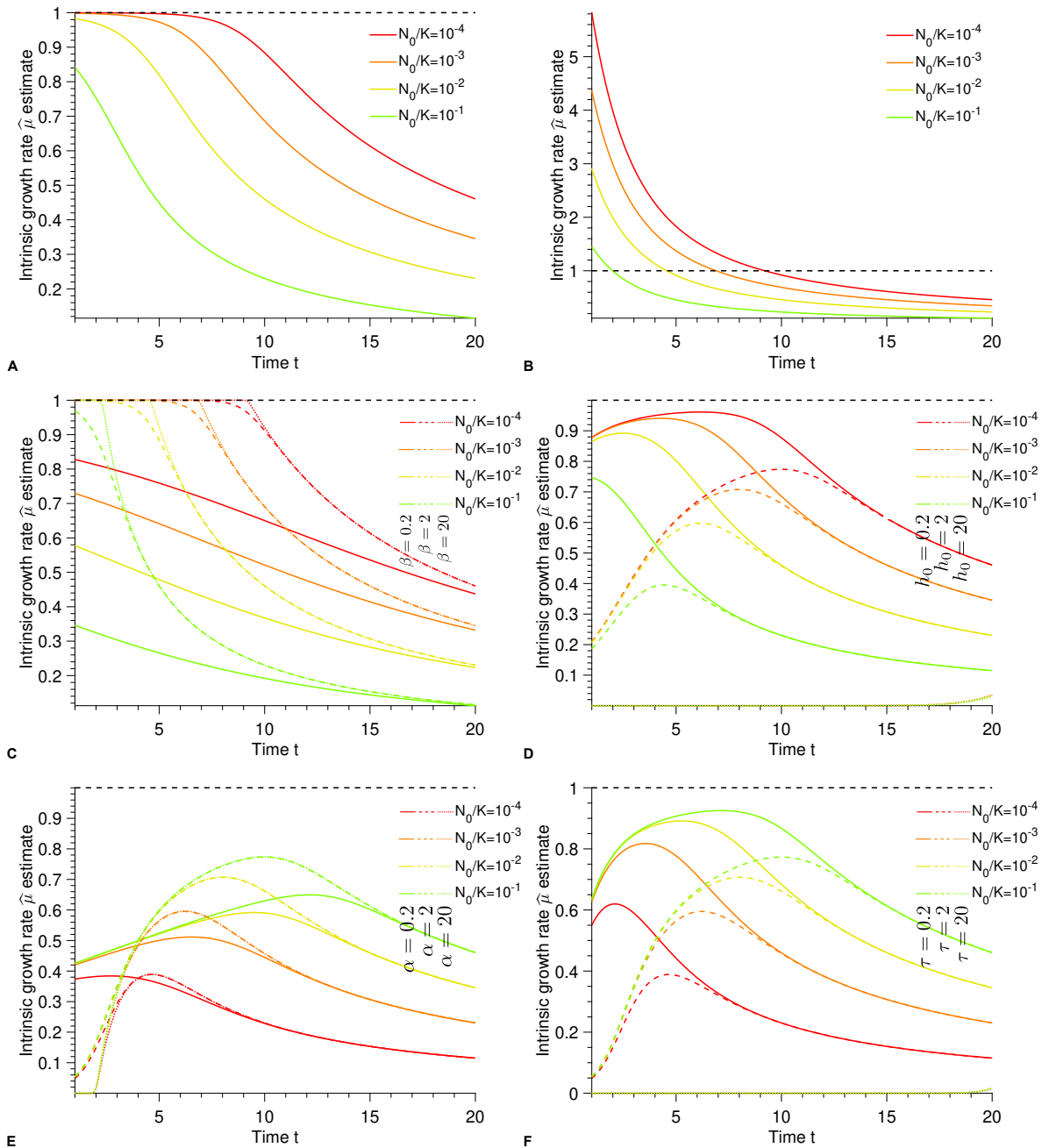


Figure S5: **Intrinsic growth rate:** From A) to F) Intrinsic growth rate $\hat{\mu}$ estimate versus parameter t for different initial population fractions N_0/K , parameters and kinetic models (A) Logistic, B) Gompertz, C) Richards, D) Baranyi, E) and F) Huang). The intrinsic growth rate is analytically estimated using the exponential hypothesis $\mu/\hat{\mu} = \ln(N(t)/N_0)/t$. The black dashed line shows the real value of μ . Parameter values: $K = 10^5$, μ , $\tau = 2$ for E) and $\alpha = 2$ for F).

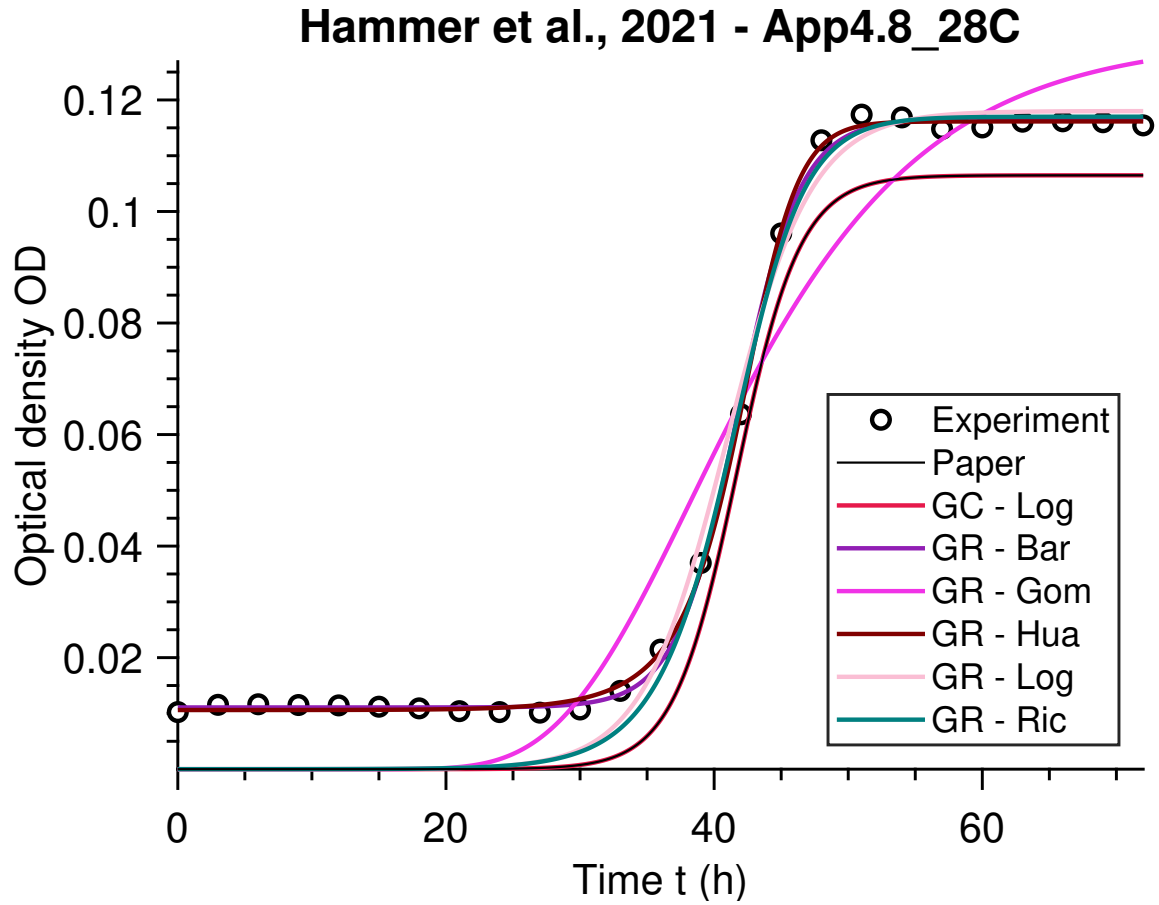


Figure S6: **Analysis of published data:** Optical density OD versus time t . The data points are fitted using different kinetic models. The black (Paper) and red (Growthcurver - Logistic (K)) lines are the same since it was the method applied in the paper.

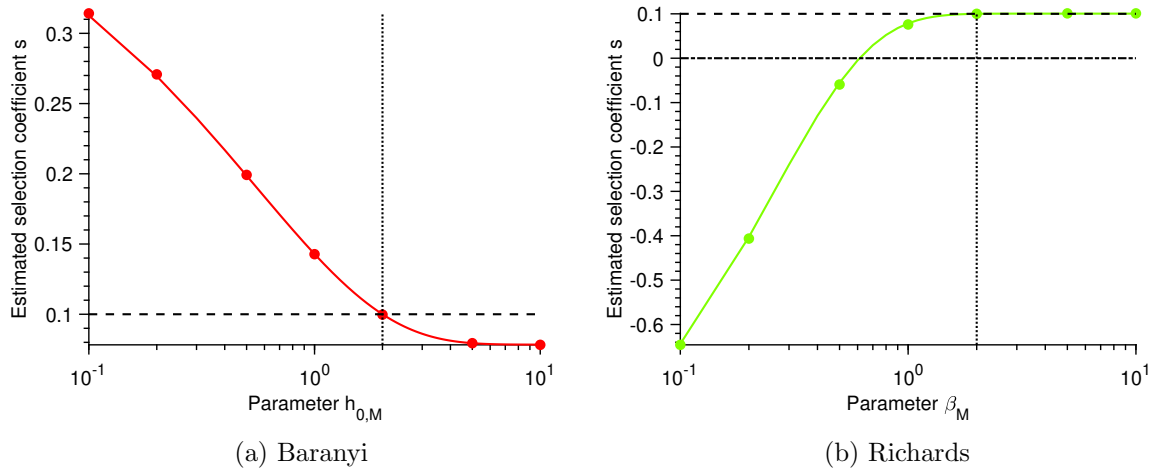


Figure S7: **Selection coefficient:** a) Estimated selection coefficient \hat{s} versus parameter h_0 for the Baranyi model. b) Estimated selection coefficient \hat{s} versus parameter β for the Richards model. In every panel, each point represents estimated values from simulated data averaged over 10^4 stochastic realizations. The solid lines correspond to the analytical predictions of the selection coefficient using those of the maximum growth rate (see Table 2.2.1 in the main text). The dashed line shows the real selection coefficient value s . The dotted line represents the configuration where the parameters of the mutant are equal to those of the wild-type (except their growth rates). The dash-dot line corresponds to the neutral case, i.e. where both the mutant and the wild-type have the same growth rate. Parameter values: $K_W = K_M = 10^5$, $\mu_W = 1$, $\mu_M = 1.1$, $s = 0.1$, $\beta_W = 2$ and $h_{0,W} = 2$. When not specified, β_M and $h_{0,M}$ have the same values as the wild-type.